CHAPTER 5

APPLICATION OF THE SIMULATION MODEL

TO LOS ANGELES SULFATE AIR QUALITY

5.1 Introduction

In order to verify our understanding of emissions-air quality
relationships, we wish to simulate the succession of sulfate air
quality patterns observed in the Los Angeles Basin over a period of
several years. In Chapter 2, it was decided that the available air
quality data would best support a simulation of monthly average sulfate
air quality during the years 1972 through 1974.

An air quality model suited to this task has been derived. Sulfur
oxides emissions in the South Coast Air Basin have been defined for
each month of that three year test period. In this chapter, the
remaining data requirements of the simulation model will be explained
and satisfied. Then the air quality model will be applied to analysis
of the Los Angeles sulfate problem, and comparisons will be drawn
between observed and predicted sulfate concentrations.

5.2 The Data Required for Model Validation

Given the long-term average air quality model derived in Chapter 3,
a simulation may be conducted to estimate the sulfate concentration
patterns appearing in the Los Angeles Basin during each month of the
years 1972 through 1974. The input data and data preparation steps
required for this simulation are:

1. Consolidation of the SO_x emissions inventory into $i = 1,2,\ldots,N_4$ source classes. A source class is composed of a group of j sources whose emissions behavior is similar except for geographic location $\underset{\sim}{X}_{o_j}$ and average emissions strength, $\overline{S}(\underset{\sim}{X}_{o_j},i)$ of each of the j members of that class.

2. Specification of effective stack height for each source class as a function of time of pollutant release.

3. Specification of the diurnal variation in source emission strength, $\omega(i,t_o)$, for each source class.

4. Specification of the initial fraction of the SO_x emissions which originated as SO_3 or sulfates, $f_{s_o}(i)$, from each source class.

5. An estimate of the maximum retention time for an air parcel in the air basin, τ_c.

6. A continuous record of hourly wind speed and direction data for each month of interest, plus the τ_c hours preceding the start of each month.

7. A sequence of hourly estimates for inversion base height for each month of interest plus the τ_c hours preceding the start of each month.

8. A function for estimating the rate of horizontal eddy diffusion in the form $(\sigma_1(t-t_o), \sigma_2(t-t_o))$.

9. Estimates of SO_2 deposition velocity, V_g; sulfate deposition velocity, V_p, and sulfate formation rate, k.

10. An estimate of the seasonal variation in sulfate background concentrations.

11. A choice of receptor cell size Δx_1, Δx_2. A review of our model derivation shows that the product of $\Delta x_3 \cdot \dfrac{h(t)}{\Delta x_3}$ cancels the need for specification of a vertical cell dimension.

12. Choice of a time step, Δt.

Acquisition or preparation of each of these data bases will be discussed in turn.

5.2.1 Emission Source Related Data

The spatially resolved SO_x emissions estimates of Chapter 4 and Appendix A2 will be used as the basis for this air quality simulation. In that emissions inventory, separate source classes were defined for nineteen classes of stationary sources and seven types of mobile sources. For air quality modeling purposes, all members of a given source class residing within a single cell of the emissions grid displayed in Chapter 4 will be summed and then treated as a single virtual source located at the center of that cell. Emissions from major off-grid sources will be located at the center of the cells that they would occupy if the grid system of Chapter 4 was extended to cover the entire South Coast Air Basin.

To further speed the air quality model calculations, it is desirable to combine as many of the small source classes as possible in order to achieve a reduced number of virtual emission points. There are, however, two constraints on this process of source class aggregation. The first constraint is purely technical. All members of each of these larger source groupings must share a similar source effective stack height, fraction sulfates originating in their exhaust, and diurnal modulation of source emission strength. The second constraint on source class recombination is largely strategic in nature. If all source classes were lumped together for air quality model calculation purposes, no information would be gained on source class contribution to air pollutant increments observed at various air monitoring stations. This latter information on source class contribution to downwind air quality is absolutely vital if emission control strategy analysis is to proceed by a means other than trial and error.

Within this air quality model application, the decision has been made to preserve the major source classification system in use for many years by the Los Angeles Air Pollution Control District. Separate SO_x source categories will be maintained for power plants, other stationary fuel combustion sources, chemical plants, petroleum industry processes, miscellaneous stationary sources, automobiles and light trucks, and other mobile sources.

In most cases, the equipment types grouped within these major headings do display similar stack heights, fraction sulfates in their

exhaust, and diurnal emissions patterns. However, the miscellaneous stationary source category is composed of a variety of disparate industrial processes, many of which have unique characteristics. Petroleum coke calcining kilns have very high effective stack heights, and a high fraction of their sulfur oxides emissions are released directly as SO_3 or sulfates. Glass furnaces have much lower stack heights, but a high fraction sulfates in their exhaust. The off-grid steel mill has a high effective stack height and a normal amount of SO_3 in its exhaust, while most remaining metals furnaces have lower effective stack heights and a lower fraction SO_3 in their effluent. Therefore, to avoid potential distortion of our results, the air quality impact of coke calcining kilns, glass furnaces, the steel mill, and metals melting furnaces each will be calculated as from a separate source class. The emissions from all remaining miscellaneous stationary sources will be lumped to form an additional source class. Then the air quality impact of these components of the miscellaneous stationary source category may be summed at each air quality receptor point in order to recover the pollutant contribution from the miscellaneous source category as a whole. A key to this source class aggregation procedure is provided in Table 5.1.

Table 4.7 in Chapter 4 was constructed in anticipation of this source class recombination scheme. It shows the weighted-average fraction sulfates in the exhaust of each of the major source class groupings that will be used for air quality model calculations. Those weighted-average values of f_{s_o} are summarized in Table 5.1.

258

TABLE 5.1

Source Class Aggregation Scheme
Used to Reduce the Number of Virtual Emissions Sources
within the Air Quality Simulation Model

Source Classes Inventoried	Aggregated Source Classes (Supplied to Air Quality Model)	Stack Parameters at Reference Conditions (a)		Fraction SO_3 in Exhaust (b)
		Stack Height H meters	Plume Rise ΔH meters	f_{SO_3} percent
Stationary Sources				
Fuel Combustion				
Electric Utilities	Electric Utilities	68.6	250.6	3.0%
Refinery Fuel Burning				
Other Interruptible Gas Customers	Other Stationary Fuel Combustion Sources	30.5	54.9	3.0%
Firm Gas Customers				
Chemical Plants				
Sulfur Recovery Plants	Chemical Plants	41.2	36.6	0.6%
Sulfuric Acid Plants				
Other Chemicals				
Petroleum Refining and Production				
Fluid Catalytic Crackers	Petroleum Refining and Production	37.2	164.6	2.8%
Sour Water Strippers				
Delayed Cokers				
Miscellaneous Refinery Processes				
Oil Field Production				
Miscellaneous Stationary Sources	Miscellaneous Stationary Sources			
Petroleum Coke Calcining Kilns	Petroleum Coke Calcining Kilns	45.7	384.4	8.4%
Glass Furnaces	Glass Furnaces	22.9	44.8	18.0%
Secondary Metals Industries (On-Grid)	Secondary Metals Industries (On-Grid)	16.8	33.5	1.0%
Primary Metals (Off-Grid Steel Mill)	Primary Metals (Off-Grid Steel Mill)	72.5	129.8	2.5%
Minerals Products				
Sewage Treatment Digesters	Other Miscellaneous Stationary Sources	10.7	21.3	2.8%
Other Industrial Processes				
Permitted Incinerators				
Mobile Sources				
Autos and Lt. Trucks - Surface				
Autos and Lt. Trucks - Freeway				
Heavy Duty Vehicles - Surface	Autos and Light Trucks	Surface mixed layer		0.3%
Heavy Duty Vehicles - Freeway				
Airport Operations				
Shipping Operations	Other Mobile Sources	Surface mixed layer		2.5%
Railroad Operations				

Notes: (a) Reference Conditions: neutral stability, ambient temperature = 18°C, wind speed = 2.77 m/sec.

(b) 1973 emissions weighted average within each source grouping shown.

In a similar fashion, Table 5.1 assigns a typical physical stack height and plume rise at reference conditions to each of these major source class groupings, based on the more detailed analysis of Table 4.9 in Chapter 4. Emphasis has been placed on most closely reproducing the stack parameters of the dominant equipment type within each of these aggregated source classes. For example, since fluid catalytic cracking units totally dominate SO_x emissions from petroleum refinery processes, the refinery process source class grouping as a whole was assigned stack parameters appropriate to fluid catalytic cracking units. These plume rise estimates at reference conditions will be adjusted hourly within the air quality model calculation in order to better reflect observed wind speed at each time step, as outlined in Appendix A4. Mobile sources are assumed to emit within the surface mixed layer of our model.

The diurnal variation of emissions from source class groupings must also be addressed. Automotive emission strength is taken to follow the weighted average of freeway and surface street traffic flows as given in Table 4.8. Power plants still occupy a single source class with diurnal variation in emission strength as given in Table 4.8. All other source groupings will be assumed to emit at an average rate independent of time of day.

5.2.2 Meteorological Data

From meteorological records, we need to prepare a time history of wind speed, wind direction and inversion base motion. The maximum

retention time, τ_c, for an air parcel within our study area must also be estimated from available records on resultant air mass transport in the Los Angeles Basin.

In Chapter 3, section 3.4.2, it was decided that transport calculations would be based on wind data acquired at the downtown Los Angeles monitoring station of the Los Angeles Air Pollution Control District. A detailed justification for that selection is contained in Chapter 3. Wind records from that monitoring site were acquired on magnetic tape from the Los Angeles Air Pollution Control District (1975a).

In Chapter 3, it was also decided that inversion base motion would be represented by a stylized diurnal cycle which passes through the measured early morning and calculated afternoon maximum mixing depths in the Los Angeles area. These two point estimates of mixing depth in the Los Angeles Basin were again obtained on magnetic tape for each day of our three year period from the files of the Los Angeles Air Pollution Control District (1975b). The data were then interpolated to form an estimated mixing depth above ground level at each hour of each day in the manner described in Chapter 3 (see Figure 3.6). In those instances where inversion base height was stated only as greater than the LAAPCD's maximum reported altitude of 1524 m (5000 ft), a mixing depth of 2032 m (6667 ft) was assumed. That value was estimated by graphing sulfate concentration against h_{max}^{-1} and then visually estimating a single mixing depth for all such events which

best preserved the already strong negative correlation between sulfate concentration and afternoon maximum mixing depth.

The National Oceanic and Atmospheric Administration (NOAA) of the U. S. Department of Commerce (1972a through 1974a) has published local climatological data summaries for their weather station located in Long Beach, California. Wind data at that station have been reduced by NOAA to form comparative summaries of scalar average and vector average wind speed. The vector average wind speeds, called resultant winds, reflect the net displacement of air masses passing that station during each month of the year. The scalar average wind speed is the average of the wind velocities computed without regard for reversals in the direction of air parcel transport. These data form an interesting preface to our discussion of τ_c, the length of time needed for trajectory integration in order to transport air parcels emitted from local sources to beyond the boundaries of our study area.

Table 5.2 shows this comparison of vector averaged and scalar averaged wind speeds at Long Beach for each month of the years 1972 through 1974. Vector averaged wind speed at that location is typically less than half of the average scalar wind speed. This circumstance results from the daily sea breeze/land breeze reversal in wind direction which causes air parcel transport to recirculate within the Los Angeles Basin. The most extreme examples of the disparity between apparent average wind speed and actual vector displacement of air parcels from their points of origin occur in the winter months. Vector averaged wind speeds are often a factor of five to ten times slower than average

Table 5.2

Monthly Resultant Wind Data
For Long Beach During the
Years 1972 through 1974

Month	Resultant Wind Speed Computed after Progressive Vector Addition of Successive Wind Observations for Each Month (miles per hour)			Scalar Average of Wind Velocity Observations (miles per hour)		
	1972	1973	1974	1972	1973	1974
January	0.4	1.0	1.0	5.6	6.4	4.8
February	0.9	1.4	1.2	5.2	6.5	5.4
March	2.5	4.3	2.5	6.0	8.2	5.2
April	2.7	2.8	3.5	6.2	8.1	5.7
May	3.4	3.2	3.1	6.9	6.4	5.7
June	3.8	3.1	2.7	7.3	6.4	5.3
July	3.0	2.9	2.7	7.1	5.8	5.4
August	2.8	2.8	2.6	6.7	6.1	5.4
September	3.2	2.6	1.6	6.8	6.2	3.3
October	2.0	2.1	2.6	5.7	5.6	5.4
November	1.3	1.5	1.9	5.5	5.1	4.9
December	2.1	0.6	0.6	6.2	3.0	5.3

Source: U.S. Department of Commerce (1972a through 1974a)

To convert miles per hour to meters per second, multiply by 0.45.

scalar wind speeds during the winter. Such persistent disparity between scalar average and resultant wind speeds is a clear indication of the need for a long-term average air quality model which can handle unsteady meteorological conditions.

The area over which we wish to compute sulfate concentrations is contained within the grid system established in Chapter 4 for displaying emission inventory results. The characteristic dimensions of that grid are defined by a square fifty miles (80.47 km) along each edge. Air masses transiting our study area may pass in and out of the boundaries of that receptor zone several times before permanently exiting the study area. But the average resultant wind speed at Long Beach just in excess of 0.9 meters per second (2 miles per hour) suggests that the typical air parcel will receive a net displacement to beyond the borders of our receptor grid within one twenty-four hour period.

While typical trajectories will clear the study area within one 24-hour period, a selection of trajectory integration time, τ_c, must be made with the intent of matching the maximum retention time for air parcels within the airshed. Therefore a simulation was constructed to estimate the fraction of trajectories computed within the assumptions of our model which would still have endpoints remaining within the 50 by 50 mile square at the end of various lengths of time.

Three critical trajectory starting locations representing major point source areas in the airshed were first isolated. The starting locations chosen were El Segundo (near two power plants and one

refinery), Los Alamitos (near two very large power plants), and a third location in the middle of the harbor refinery complex (near Stauffer Chemical). Next a trial value for τ_c was assumed, for example τ_c = 24 hours. Trajectories of duration τ_c starting from these locations and ending at each hour of each day of the years 1972 through 1974 were estimated from wind data apparent at the LAAPCD's downtown Los Angeles monitoring station. Then the fraction of trajectory end points remaining within the 50 by 50 mile square after τ_c hours of pollutant transport could be determined by inspection.

As this trajectory screening process is repeated for successively larger values of τ_c, the progression of events is as illustrated in Figure 5.1. Within the first few hours of trajectory integration, large numbers of air parcels released during high speed wind events are advected out of our study area. True to our expectations, the centroid of the average air parcel released is out of the 50 by 50 mile square at the end of a 24 hour period.

As τ_c is extended further in an attempt to completely eliminate trajectory end points from our grid, we face the prospect of diminishing returns to increased computational effort. A truncation point for trajectory integration must be established unless unreasonable amounts of computing time are to be spent extending the integration of hundreds of off-grid trajectories in order to search for a few stagnating trajectories which are still within the receptor grid.

For the purposes of this study, a value of τ_c will be selected such that 95% of the end points of trajectories of age τ_c originating
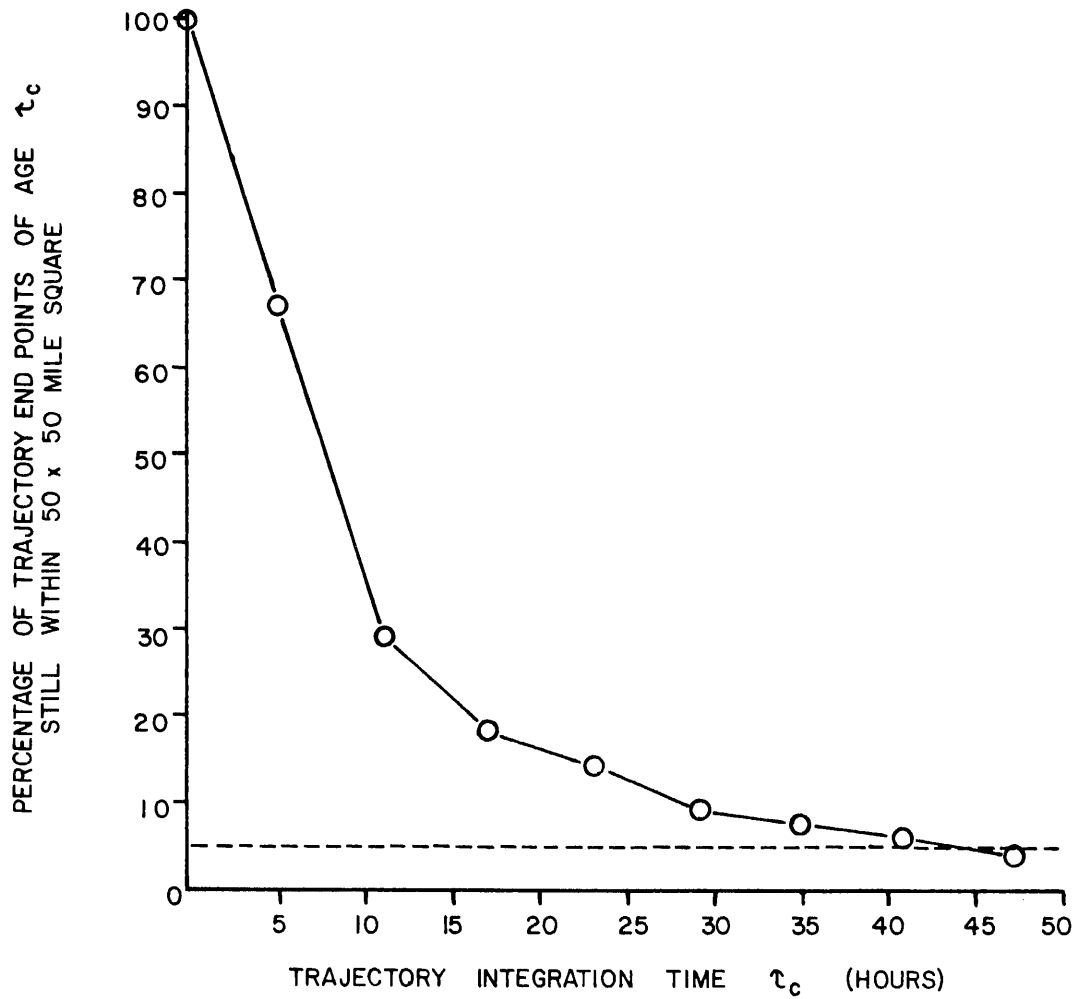
FIGURE 5.1

Retention of Air Parcels Released from Major
Point Source Locations in the Los Angeles Basin.

from major point sources will be off-grid at the end of trajectory integration. From Figure 5.1 we find that that value of $\tau_{95\%} \approx \tau_c$ corresponds to a trajectory integration time of two days for the major source locations and receptor grid of interest to us.

It should be noted that this selection does not mean that 5% of the material contributing to observed SO_x concentrations has been neglected. That is because when selecting a value for τ_c we focused only on the oldest air parcels in the airshed for any assumed value of τ_c. The retention of air parcels of all ages τ_c or less is given by the area under the curve of Figure 5.1. By truncating the trajectory integration at $\tau_{95\%} \approx \tau_c$, we have removed an amount of pollutant mass approximately equal to the area of the tail of that declining curve beyond $\tau_{95\%}$ equals two days.

5.2.3 Estimation of Air Parcel Diffusive Displacement

Small scale turbulence in the atmosphere acts to influence fluid particle transport beyond that computed from trajectories based on mean wind speed and direction alone. We wish to estimate the rate at which this process of eddy diffusion occurs over the Los Angeles urban area so that diffusive displacements may be imparted to individual fluid particles within our simulation model.

The cross-wind standard deviation of a puff or plume, σ_y, is often used to specify the horizontal dispersion of pollutant material about its center of mass. A theoretically satisfactory way to predict the rate of plume spread in the atmosphere is still in its formative stages.

Therefore values of the growth in σ_y with time or distance from the point of pollutant release are usually obtained from field measurement programs. Successive estimates of the dispersion parameter, σ_y, are calculated from experimental results and then organized in terms of simultaneously occurring indices of atmospheric turbulence. Plume dispersion experiments have been tabulated in terms of atmospheric "stability classes"; the rapidity of horizontal fluctuations in wind direction; the standard deviation of fluctuations in the angle of horizontal wind direction, and combinations of measured wind fluctuation and vertical atmospheric stability (McElroy and Pooler, 1968).

The most commonly encountered atmospheric dispersion estimates in use today rely on Pasquill-Gifford stability classes to predict plume spreading (see Pasquill (1961), Gifford (1961), Turner (1969)). The popularity of that system arises from the fact that it requires only readily available measurements of surface wind speed, solar radiation intensity and cloud cover in order to dictate selection of one of six stability classes. Each stability class is paired with expressions for estimation of the rate of plume spreading as a function of distance downwind from the source.

Turner (1969) summarizes some important background information on the experiments which form the basis for the Pasquill-Gifford dispersion estimates:

> "These methods will give representative indications of
> stability over open country or rural areas, but are less
> reliable for urban areas. This difference is due primarily
> to the influence of the city's larger surface roughness
> and heat island effects upon the stability regime over
> urban areas...."

Since our simulation model is to be applied to the atmosphere over one
of the world's most extensive continuous urban areas, dispersion
estimates specific to an urban airshed will be sought.

Figure 5.2 shows a series of experimental results for horizontal
dispersion of inert tracer material over the urban area of St. Louis
(McElroy and Pooler, 1968). The data are organized in terms of travel
time downwind, which is particularly convenient for use in our simula-
tion model. Dispersion data have been analyzed within four classes
based on the standard deviation of wind direction fluctuations, σ_θ,
and bulk Richardson number, Ri_B. The actual separation of the data
appears to fall into only two major classes. Dispersion under stable
atmospheric conditions (the o's) is distinctly different from the
grouping of all remaining observations on σ_y.

When the data of McElroy and Pooler (1968) are compared to
estimates of σ_y and σ_z[1] given by the Pasquill-Gifford curves, it is
found that

> "...best-fit lines for σ_y and σ_z for the St. Louis data
> are everywhere larger than those for the open-country
> counterparts. When extrapolated to longer downwind
> distances, the best-fit lines for σ_y approach their
> counterparts; those for σ_z generally approach counter-
> parts of stability one class higher." (McElroy and Pooler,
> 1968).

The need to extrapolate McElroy and Pooler's (1968) data to greater
downwind distances should be emphasized. From Figure 5.2 it is seen

---

[1] σ_z is the standard deviation of plume spread in the vertical dimension.
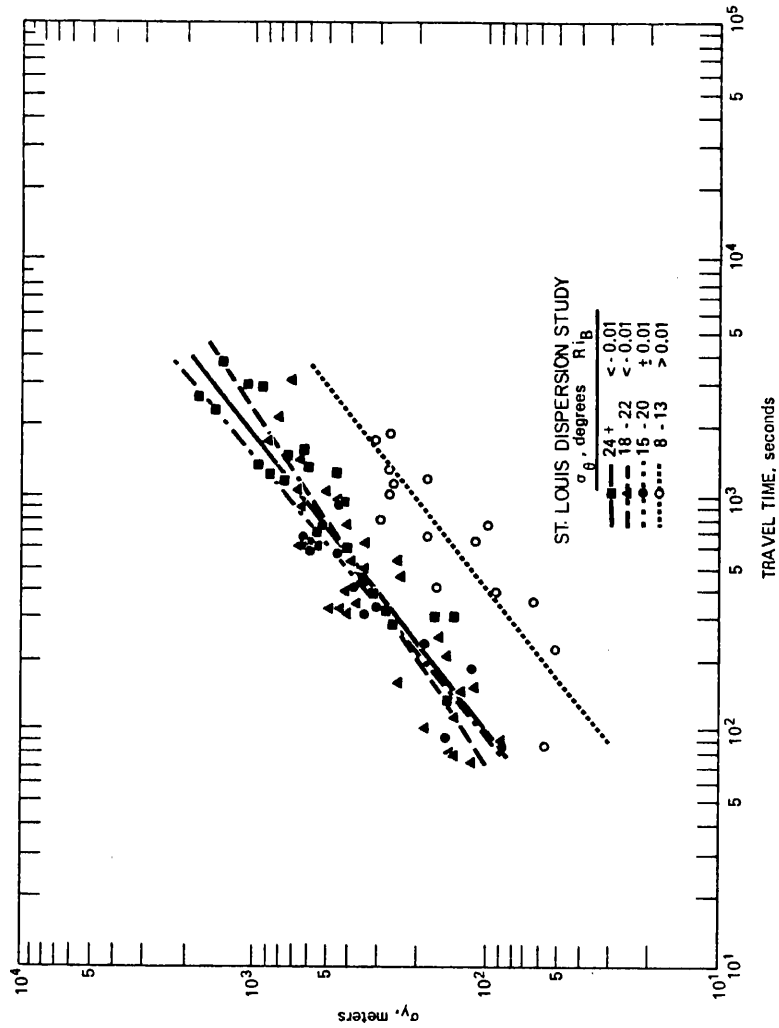
FIGURE 5.2

Cross-wind standard deviation of tracer material as a function of travel time in
terms of standard deviation of wind direction fluctuations (σ_θ) and bulk Richardson number (Ri_B).
(From McElroy and Pooler, 1968)

that experimental results are available for only the first hour or so of downwind travel.

A limited amount of longer distance experimental data have been collected for dispersion over the Los Angeles Basin from the work of Drivas and Shair (1975) and Shair (1977). These data are displayed in Table 5.3, along with a few descriptive notes about the conditions of each experiment.

In Figure 5.3, the Los Angeles Basin data are plotted alongside the results of the St. Louis Dispersion Study. It is seen that the Los Angeles data fall within the envelope established by the extension of McElroy and Pooler's (1968) lines of best fit for their most turbulent and least turbulent atmospheric conditions.

A procedure for extending the results of McElroy and Pooler to include the Los Angeles data is sought. Two problems arise. First, if the data sets were pooled, the St. Louis data would dominate the statistics of the results as they are far more numerous. In contrast, we wish to emphasize the Los Angeles data because they represent transport over the scale of the particular urban air basin of interest to us rather than short distance transport downwind of sources in another city. Secondly, when the Los Angeles data are viewed in terms of the experimental conditions under which they were taken, there is no clear evidence that a separation of the data into groups of more or less "stable" atmospheric conditions (in the Pasquill-Gifford sense) would be supportable. About all that can be said is that the

TABLE 5.3

Values of the Dispersion Parameter, σ_y, Calculated from Experiments in the Los Angeles Basin

Test Number	Date	Time of Day at which Traverse was taken PST	Wind velocity u m/sec	Downwind Distance at Point of Traverse x, km	Downwind Travel Time to Point of Traverse t sec	σ_y m	Stability Class Estimated by Pasquill-Gifford Method	Remarks
Long Beach[a] No.2	10/11/74	3:23-3:45 PM	2.5	15	6000	844	B-C[c]	Trajectory Entirely Over Urban Area
Long Beach[a] No.3	10/17/74	3:14-3:35 PM	3.0	15	5000	2460	B-C[c]	Trajectory Entirely Over Urban Area
Long Beach[a] No.4	10/25/74	2:08-3:12 PM	4.5	15	3333	769	B-C[c]	Trajectory Entirely Over Urban Area
Long Beach[a] No.5	10/30/74	2:39-3:41 PM	5.5	15	2727	864	C-D[c]	Trajectory Entirely Over Urban Area
Long Beach[a] No.6	10/07/74	2:24-2:45 PM	4.5	15	3333	1220	B-C[c]	Trajectory Entirely Over Urban Area
Long Beach[a] No.6	11/07/74	2:53-3:11 PM	6.0	15	2500	534	C-D[c]	Trajectory Entirely Over Urban Area
Long Beach[a] No.6	11/07/74	3:50-4:10 PM	5.0	15	3000	637	C-D[c]	Trajectory Entirely Over Urban Area
Land-Sea Breeze (b) No.6	9/13/77	1:04-1:48 PM	2.6	43	16800	3260	Mixed[d]	Trajectory 90% Over water; 10% Over Urban Area
Land-Sea Breeze (b) No.6	9/13/77	2:26-3:12 PM	2.6	43	16800	2062	Mixed[d]	Trajectory 90% Over Water; 10% Over Urban Area
Land-Sea Breeze (b) No.6	9/13/77	3:30-4:27 PM	3.4	67	19800	6205	Mixed[d]	Trajectory 60% Over Water; 40% Over Urban Area
Land-Sea Breeze (b) No.6	9/13/77	4:02-4:38 PM	3.4	88	26100	7064	Mixed[d]	Trajectory 50% Over Water; 50% Over Urban Area

(a) SF_6 Release from Power Plant Stack at Alamitos Bay; Reference Drivas and Shair (1975)
(b) SF_6 Release beginning at 9:00 AM, from Shipping Lanes at Sea; Reference Shair (1977)
(c) As estimated by Drivas and Shair (1975)
(d) Stability Class Could Have Ranged Between Class A and Class D During Different Parts of Trajectory; Release Made at Sea Under Cloudy Conditions, While Later Part of Trajectory Occurred Over Land Under Condtions of Strong Incoming Solar Radiation.
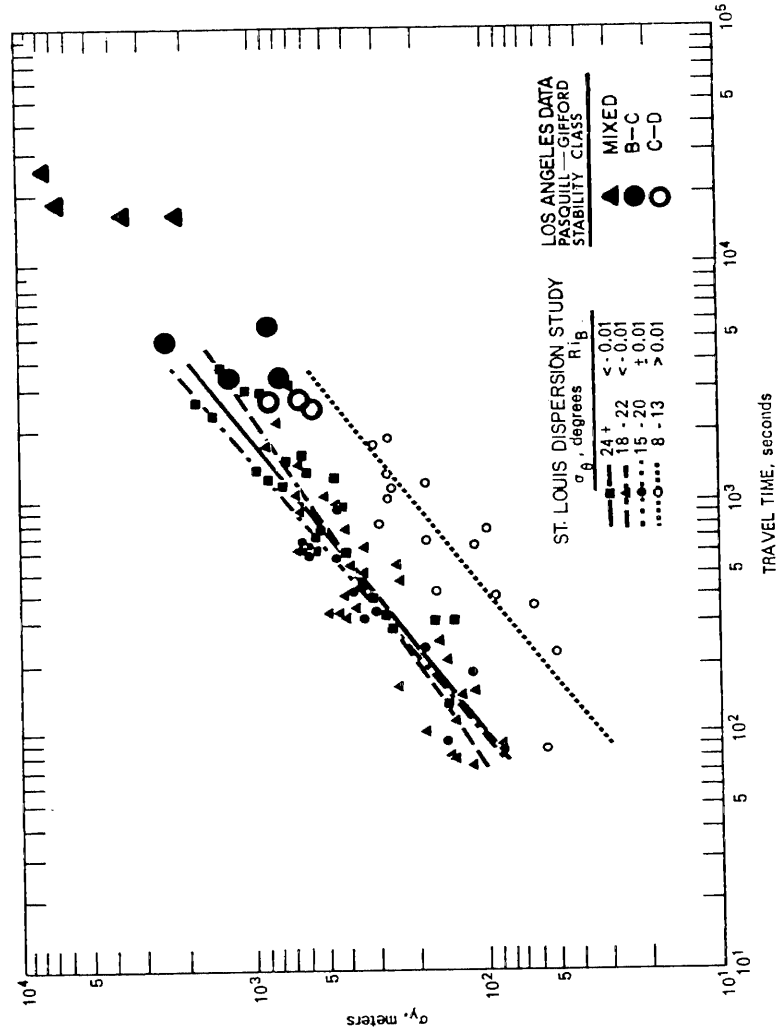
FIGURE 5.3

Cross-wind standard deviation of tracer material as a function of travel time in terms of standard
deviation of wind direction fluctuations (σ_θ) and bulk Richardson number (Ri_B), from McElroy
and Pooler (1968), plus Los Angeles data from Drivas and Shair (1975) and Shair (1977), organized
by Pasquill-Gifford stability classes.

Los Angeles results fall within the band formed by the extension of McElroy and Pooler's observations.

Therefore, the following approach was adopted. The Los Angeles data will be reduced to form a single function relating lateral plume spread to downwind travel time. That function will be expressed as a simple power law, similar to the curves in Figure 5.2, as follows:

$$\sigma_y = bt^a \tag{5.1}$$

where

σ_y is the horizontal standard deviation of plume spread about its centerline.

t is travel time downwind.

a and b are fitted constants.

The slope of the curve relating σ_y to travel time ("a" in equation 5.1) will be estimated graphically from the slope of the band defined by McElroy and Pooler's most turbulent ($\sigma_\theta = 24°+$) and least turbulent ($\sigma_\theta = 8°-13°$) conditions. Then the constant b in expression (5.1) will be fitted to the Los Angeles data alone by least squares regression techniques. The following estimates for the rate of horizontal plume dispersion over Los Angeles result:

$$\sigma_y = 1.73\ t^{0.80} \tag{5.2}$$

for σ_y in meters and time in seconds, or

$$\sigma_y = 0.75\ t^{0.80} \tag{5.3}$$

for σ_y in miles and time in hours. Equation (5.2) is graphed alongside the available data in Figure 5.4.
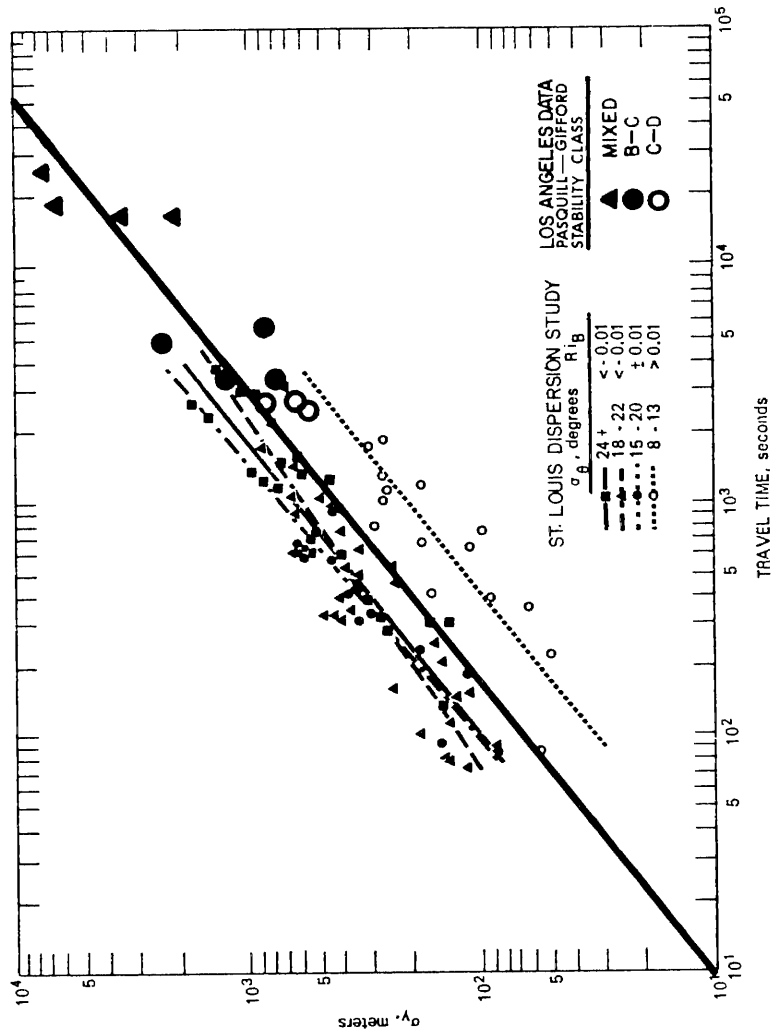
FIGURE 5.4

Cross-wind standard deviation of plume spread showing the function for $\sigma_y(t)$ fit to the Los Angeles data (heavy solid line). Function was estimated by linear regression after having transformed the time axis as $t^{0.8}$.

That explains why higher valued observations seem to dominate the result on this log-log plot.

Long distance trajectories will undoubtedly encounter changing atmospheric turbulence levels while in transit. The use of a single expression fitted to data from a variety of observational conditions in the field should help to yield results which do not stray greatly from a typical mixture of atmospheric conditions encountered by long distance trajectories in Los Angeles.

In order to introduce these estimates for horizontal dispersion into our simulation model, one further approximation must be made. It is assumed that an expanding puff in the atmosphere remains symmetric, with equal downwind and crosswind standard deviations at any single time. In that case, $\sigma_y = \sigma_1 = \sigma_2$, and the data on (σ_1, σ_2) required by our air quality model derivation may be supplied by equations (5.2) or (5.3). In an open atmosphere characterized by both vertical and horizontal wind shear, this symmetry may not be preserved. Vertical wind shear could cause an air parcel shaped like an upright circular cylinder to bend over while vertical mixing acts to render the ground level profile of the air parcel into an ellipse. Horizontal wind shear could tear an expanding puff into separate fragments. But field data on long distance puff expansion upon which to base a more complex dispersion analysis are unavailable for Los Angeles.

5.2.4 <u>Estimation of Pollutant Dry Deposition Velocities and Chemical Reaction Rates</u>

From the mass balance calculations of Roberts (1975; see Figure 2.17) it is clear that estimation of pollutant deposition rates is critical to a correct simulation of Los Angeles sulfur oxides air

quality levels. Roberts estimated that dry deposition of SO_2 and sulfates removed half of the sulfur oxides emitted during his day of interest before those air parcels exited the Los Angeles area.

Dry deposition of sulfur dioxide has been studied under both laboratory and field conditions. From these studies and from theoretical considerations, it is found that the flux of sulfur dioxide to the earth's surface is limited by a resistance due to the rate of diffusion in the atmosphere plus a resistance due to the condition of the receiving surface material. This relationship is expressed as follows (Garland, 1974):

$$r = r_a + r_b + r_s \qquad (5.4)$$

where

r	is total resistance to SO_2 deposition in sec/cm.
r_a	is aerodynamic resistance calculated from momentum transport considerations.
r_b	is an aerodynamic resistance arising from the differences between mass transfer and momentum transfer processes.
r_s	is surface resistance.

Deposition velocity is related to total resistance to deposition by

$$V_g = \frac{1}{r} \qquad (5.5)$$

Large bodies of water may behave as a near perfect sink for SO_2 (Liss, 1971; Spedding, 1972), and gas phase resistance would control the rate of pollutant removal. But most measurements of V_g show a reduced rate of SO_2 deposition that is significantly affected by surface conditions. Typical examples of sulfur dioxide deposition velocity onto natural surfaces are given in Table 5.4.

TABLE 5.4

SULFUR DIOXIDE DEPOSITION VELOCITY MEASURED OVER VARIOUS SURFACE TYPES

Surface Material	Time of Year	Mean SO_2 Deposition Velocity vg (cm/sec)	References
Short Grass	March – June	0.55	Garland (1974)
Medium Grass (radioactive tracer)	June – November	1.19	Garland (1974)
Medium Grass (gradient method)	November – January	0.77	Garland (1974)
Bare Calcareous Soil	February – March	1.1	Garland (1974)
Fresh Water – pH 8	April – June	0.46	Garland (1974)
Forest (Pine)	June	<2	Garland (1974)
Grass	Summer	0.8	Shepherd (1974)
Grass	Autumn	0.3	Shepherd (1974)
Grassland (light wind)		0.7 ± 0.1	Owers and Powell (1974)
Water (light wind)		0.9	Owers and Powell (1974)
Grassland (windy conditions)		2.6 ± 0.3	Owers and Powell (1974)
Grassland (low wind)		0.7 ± 0.1	Owers and Powell (1974)
Water (low wind)		0.5 ± 0.1	Owers and Powell (1974)

278

Typical values for SO_2 deposition velocities recommended for mass

balance calculations over grassland and water by Garland (1974) and

by Owers and Powell (1974) range from 0.7 cm/sec to 0.9 cm/sec.

Studies of SO_2 deposition averaged over the surface of urban

areas are quite rare. Laboratory studies of deposition to building

materials and Los Angeles area soils have been conducted by Judeikis and

Stewart (1976). These surveys show that concrete and stucco are

excellent sinks for SO_2; that deposition rates to Los Angeles area

soils are not greatly different from the average of results reported

for other natural surfaces, while asphalt surfaces were found to show

an extremely high resistance to SO_2 deposition. The only attempt to

integrate deposition velocities over an entire urban area that we have

found is due to Chamberlin (1960). He estimated a deposition rate

of 0.7 cm/sec for SO_2 removal during a London pollution episode.

Following the mass balance work of Garland (1974) and Chamberlin

(1960), it will be estimated that the deposition velocity for SO_2

to the surface of the Los Angeles Basin and coastal waters is about

0.7 cm/sec. However, it has been noted by Judeikis and Stewart (1976)

that a surface's ability to take up SO_2 may become saturated, and that

Los Angeles soils could become saturated within as little as eleven days

under unfavorable conditions. Judeikis and Stewart (1976) also show

that such saturated surfaces can be regenerated, for example, by a

water wash or by exposure to ammonia. This process of saturation and

regeneration could have a seasonal dependence. If so, that seasonal

dependence would modulate both SO_2 removal rates, and (indirectly)

atmospheric sulfate concentrations. A field study to explore the question of possible seasonal dependence in Los Angeles area SO_2 deposition velocity should be a high priority for those seeking to understand the South Coast Air Basin sulfur cycle.

Dry deposition of atmospheric aerosols is controlled by the size distribution of the particulate matter and fluid mechanical consider-ations in the surface layer next to the ground. Large particles of an aerodynamic diameter greater than ten microns settle very rapidly under the influence of gravity or deposit by inertial impaction. Small particles of aerodynamic diameter less than 0.01 microns deposit rapidly by diffusing to the earth's surface. A minimum in the deposition rate for particulate matter exists in the size range 0.1 to 2.0 microns aerodynamic diameter. In that range, neither atmospheric process is efficient at removing aerosol particles. This dependence of particulate deposition rate on aerosol size is illustrated in Figure 5.5 from theoretical calculations performed by Davidson (1977).

The size distribution for Los Angeles area sulfate aerosols has been measured by Hidy et al. (1975). Those data show that sulfate mass in the Los Angeles atmosphere is strongly peaked in the accumulation mode with a mass median diameter of about 0.5 microns. From Figure 5.5 we see that particles of that size should have a dry deposition velocity of about 0.02 to 0.03 cm/sec. Integration over the entire sulfate size distribution gives approximately the same value. Davidson (1977) attempted to measure the rate of sulfate dry deposition in the Los Angeles area. In spite of measurement sensitivity problems, it was

280
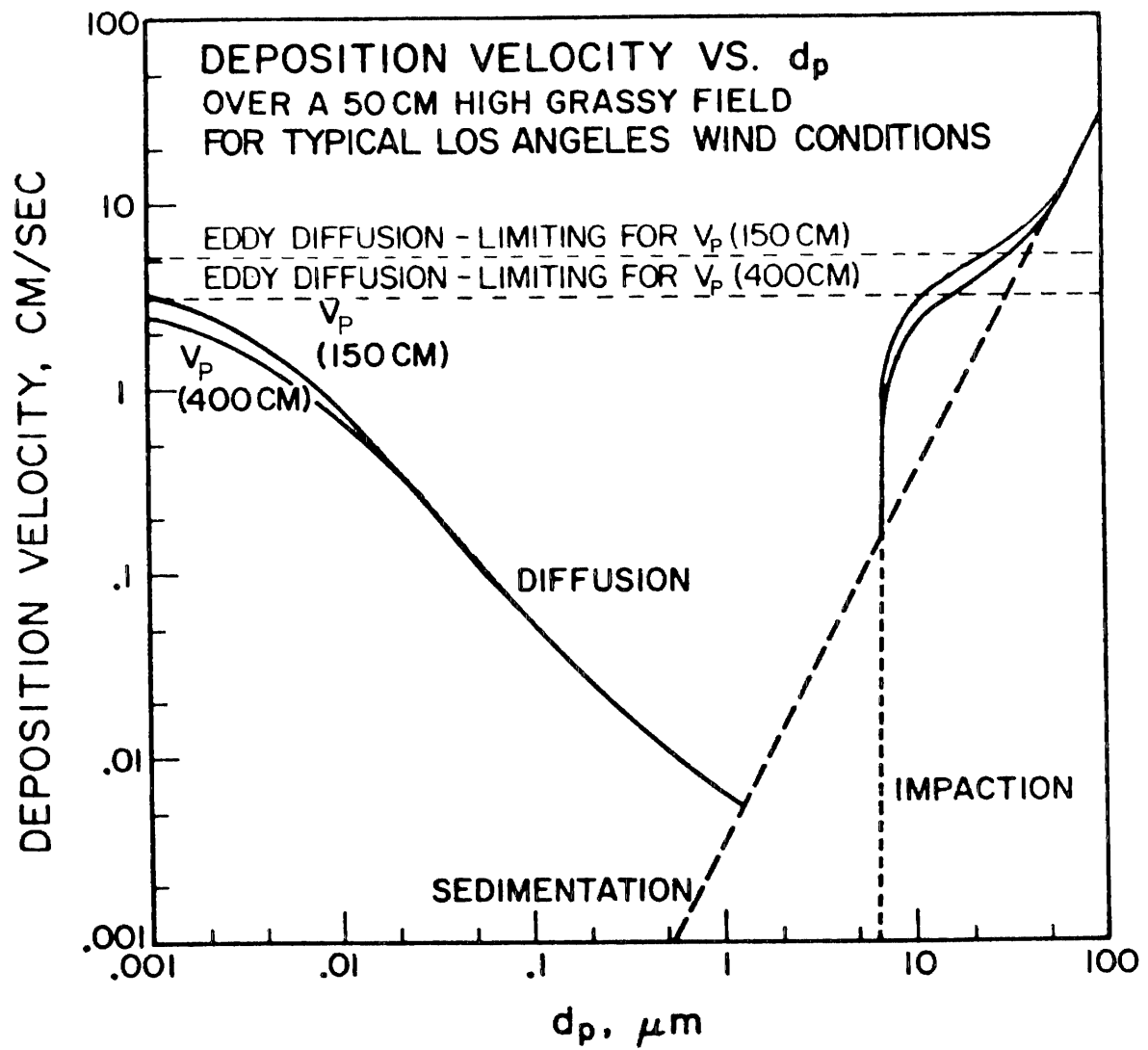
FIGURE 5.5

Calculated values of deposition velocity as a function of particle
size for heights of 150 cm and 400 cm above the ground, for a field of
Avena fatua, wild oat grass. Particle density is assumed to be 1 g/cm^3.
(From Davidson,1977).

still possible to confirm that local sulfate deposition velocities lie in the range 0.01 to 0.1 cm/sec.

Following the practice of Garland (1974), a value for particulate sulfate dry deposition of 0.03 cm/sec will be assumed. That value implies a time scale for removal of sulfate particles by dry deposition which is on the order of several weeks. In contrast, our estimate for SO_2 dry deposition of 0.7 cm/sec is more than a factor of twenty higher, yielding a half life for SO_2 removal at the ground which is on the order of days. As a result, even a substantial percentage uncertainty in sulfate dry deposition velocity can be tolerated without expecting significant impact on the results of the atmospheric mass balance which is embedded within our air quality model calculations.

In light of the complexity of the chemical reactions possible, it was decided in Chapter 2 that chemical conversion of SO_2 to form sulfates will be modeled as a slow pseudo-first order reaction. Emphasis will be placed on solving for the overall SO_2 oxidation rate and on identifying any seasonal trend in oxidation rate that may guide future theoretical investigations.

Pseudo-first order rate constants for SO_2 oxidation to form sulfates in the Los Angeles atmosphere have been measured by Roberts (1975). It was found that SO_2 oxidation rates varied from 1% to 15% per hour under photochemically active daylight sea breeze conditions. These measurements provide the range within which an average conversion rate is likely to be found.

The summertime peak in the ratio of sulfate to total sulfur oxides established in Chapter 2 suggests that there is a seasonal dependence in SO_2 oxidation rate in the Los Angeles atmosphere. As was the case with Roberts' (1975) reaction rate experiments, it will be necessary to solve for the apparent average SO_2 oxidation rate within any averaging time by a process of iteration. A trial value of the reaction rate, k, will be assumed for a given month. Next the air quality model will be exercised to generate sulfate concentration predictions throughout the airshed. Then predictions at a large number of monitoring sites will be compared to observations, and a second trial value for k will be assumed.

Estimation of a seasonal trend in SO_2 oxidation rate is a tightly constrained process in spite of the fact that values of k must be obtained by iteration. That is because the system being simulated is highly over-determined. The value of k which solves the chemical reaction equations must result in sulfate air quality predictions which match observations at a large number of air monitoring sites. Certain relationships between sulfate and total sulfur concentrations must be satisfied within a model which conserves sulfur and which does not provide any means for adjustment of total sulfur concentration predictions. A prior estimate of the likely range of values for k exists. The only parameter in the model with any freedom of adjustment, k, must simultaneously satisfy a huge system of equations or inequalities. If the model is failing to deliver reasonable concentration predictions in both time and space, no small adjustment to the value of k is likely to hide that fact.

A further check on the accuracy of the chemical modeling approach is provided by reference to the details of Roberts' (1975) experiments. The bulk of Roberts' experiments were conducted during the month of July 1973, which is one of the months which will be included within our simulation. Roberts' pseudo-first order rate constant data for July 1973 are listed in Table 5.5. The average value of k from those experiments was just under 8% per hour. A value of k equal to 8% per hour will be used to test the air quality model without freedom of adjustment for the month of July 1973[2]. One warning concerning this test is in order, however. While the calculation methods for reduction of Roberts' data differ greatly from the concentration prediction scheme of our simulation model, the underlying physical assumptions of both this study and those experiments are the same. Air parcel trajectories containing sulfur oxides are transported in a well mixed layer beneath an inversion while first order chemistry and pollutant dry deposition processes proceed to alter sulfate and total sulfur concentrations. The deposition velocity assumptions used in both studies are similar (although not identical). It is therefore possible that confirming conclusions could be reached by the process of committing identical conceptual errors. In spite of that possibility, the use of measured

---

[2]As in any iterative process, a tolerance limit must be set within which the solution being sought will be accepted as having been achieved. Within this air quality simulation, we hope to solve for monthly average values of k to within the nearest 1% per hour or twenty-five percent of full scale, whichever is less (e.g. at reaction rates below 2% per hour we will work in 0.5% per hour increments; below 1% per hour we would work in 0.25% per hour increments). For that reason, the average of Roberts' data is rounded to the nearest whole percentage point.

TABLE 5.5

Pseudo-First Order Rate Constants for SO_2 Oxidation
in the Los Angeles Atmosphere
Measured from Trajectories Terminating at Pasadena
During July 1973

Date (1973)	Trajectory Starting Location	Time of Trajectory Arrival at Pasadena (PST)	k (% hr^{-1})
July 10	El Segundo	1300	1.2 ± 0.9
	El Segundo	1400	3.0 ± 1.7
	El Segundo	1500	10.0 ± 5.7
	El Segundo	1600	14.6 ± 8.9
July 25	Alamitos Bay	1400	12.1 ± 2.0
	El Segundo	1500	8.6 ± 3.4
	El Segundo	1600	10.3 ± 2.9
July 26	Alamitos Bay	1200	5.2 ± 4.2
	Alamitos Bay	1300	5.1 ± 3.0
	Alamitos Bay	1400	8.1 ± 8.1
	Alamitos Bay	1500	4.6 ± 1.7
Range for Month of July 1973			1 to 15
Average			7.53

Source: Roberts (1975)

values of k in the simulation for July 1973 provides as stringent a
test as possible for most aspects of our simulation model.

July represented the peak month for the ratio of sulfate to total
sulfur at most monitoring sites during the year 1973. Therefore it is
expected that our estimate of an 8% per hour average conversion rate
for that month will be among the highest average rates determined as
a result of model calculations.

5.2.5 Estimation of the Seasonal Variation in Sulfate Background Air Quality

In Chapter 2 it was shown that Los Angeles sulfate air quality
is elevated above background sulfate concentrations observed at remote
locations in all surrounding directions. Since most new air masses
entering the South Coast Air Basin are of marine origin, assumptions
concerning background concentrations supplied to air quality model
calculations should reflect the marine air monitoring data.

Observations on sulfate concentrations at San Nicolas Island were
examined in Table 2.1 and Figure 2.2. These data show that sulfate
concentrations do fluctuate in the marine environment off the
Southern California Coast. Unfortunately, data sufficient to dictate
the seasonal pattern in sulfate concentrations in incoming marine air
for each month of the period 1972 through 1974 are unavailable to us.
Instead, all that is available is a set of data at San Nicolas Island
which is representative of the summer and fall of the year 1970.

However, from Figure 2.10 it is seen that every monitoring station for which we have a continuous record of sulfate air quality over the period 1972 through 1974 shows a similar seasonal trend in sulfate concentrations. That is even true of the CHESS station at Vista, located outside of the South Coast Air Basin in Northern San Diego County. While the Vista monitoring station is affected by local SO_x emissions sources to a certain degree, its concentration measurements more closely approach background levels than at any other site offering comparable data on seasonal trends.

The approach adopted in this study for estimation of sulfate background concentrations on a month by month basis is as follows. The San Nicolas Island data of Hidy, et al. (1974) will be used to set the magnitude of the average sulfate background concentrations encountered during the summer and fall of the year. Then that average will be modulated by the seasonal trend in sulfate concentrations observed at Vista.

The constant of proportionality between Vista and San Nicolas Island was estimated by examining all sulfate concentration measurements taken at both locations during the period July through October of each year of record. That time interval was set by the extent of Hidy, et al.'s (1974) sampling program. The data falling within those time periods were averaged separately at each location. The seasonally adjusted mean at San Nicolas Island was found to be 40% of the average value observed at Vista. Therefore the sulfate background concentra- tion estimates for each month of our three year period will be based

on 40% of the average sulfate concentrations observed at Vista for
that month. This time sequence of background sulfate concentration
estimates is listed in Table 5.6.

5.2.6 Selection of Time Step and a Receptor Cell Size

Selection of time step and receptor cell size should be
considered simultaneously. The fundamental question at hand is:
"Will enough particles per cell be introduced into the model to obtain
a smooth stable estimate of pollutant concentrations?"

For economic reasons, one wishes to take relatively large time
steps in order to speed the process of trajectory and chemical integra-
tion. In an opposing fashion, one prefers small receptor cells in
order to more closely define the shape of pollutant pattern contours.
If these two goals are pursued to the extreme, computed voids will
appear in the middle of zones of significant pollutant concentration.
This is due to the presence of receptor cells which are too small to
have acquired a statistically significant number of pollutant particles.

The largest time step that can be taken in our simulation model
without discarding useful data is a time step of one hour in duration.
That is the fundamental time scale of the wind data which are available
to us. Any shorter time step would have to be supported by additional
synthetic wind data gained from an interpolation scheme. Therefore
the implications of using a time step of one hour will be explored.

The time horizon for trajectory integration, τ_c, has already been
set at 48 hours. For the case of a one hour time step, 34560 trajectory

TABLE 5.6

Tabulation of Estimated Sulfate
Background Concentrations
for the South Coast Air Basin

(in $\mu gm/m^3$ as SO_4^-)

Month	1972		1973		1974	
	Vista	Background Estimate at 40% of Vista	Vista	Background Estimate at 40% of Vista	Vista	Background Estimate at 40% of Vista
January	6.03	2.41	5.87	2.35	6.78	2.71
February	11.07	4.43	4.98	1.99	6.50	2.60
March	14.12	5.65	3.28	1.31	7.21	2.88
April	8.03	3.21	6.54	2.62	6.43	2.57
May	9.78	3.91	10.32	4.13	9.84	3.94
June	16.12	6.45	11.39	4.56	8.55	3.42
July	8.14	3.26	19.25	7.70	7.76	3.10
August	11.73	4.69	17.71	7.08	12.35	4.94
September	9.16	3.66	14.02	5.61	13.98	5.59
October	7.91	3.16	11.03	4.41	12.17	4.87
November	4.90	1.96	6.66	2.66	7.40	2.96
December	5.75	2.30	7.93	3.17	4.87	1.95
Unweighted Mean		3.76		3.97		3.46

Note: Background sulfate concentrations are estimated from the seasonal
trend in sulfates observed at Vista, scaled to the level of the
average sulfate concentrations measured at San Nicolas Island.
Sulfates at Vista during the months of July through October
averaged 12.15 $\mu gm/m^3$ (3 year mean) versus an average of
4.9 $\mu gm/m^3$ at San Nicolas Island in that season of the year (see
Table 2.1). Background sulfate concentrations at San Nicolas
Island are approximately 40% of those at Vista, our most remote
site with enough data to estimate seasonal trends in background
concentrations.

end points would be counted per source as separate particles by the model when computing a monthly average pollutant concentration.[3] The area under the air parcel retention probability curve of Figure 5.1 can be integrated graphically and used to estimate the fraction of the particles released which would be likely to be counted within the 50 by 50 mile square emissions grid. It is found that about 25.5% of the 34,560 particles associated with a source at one of these major point source locations would contribute to particle counts within that 50 by 50 mile square. That translates into 8813 particle counts per source per month on the average within the 50 by 50 mile square for those critical release points.

Choice of a receptor cell size with the same dimensions as the 2 mile by 2 mile (3.22 km by 3.22 km) squares which form the emissions grid would be convenient, although not necessary. Within the 50 by 50 mile square, 625 such receptor cells would be defined. At 8813 particle counts within that zone of 625 receptor cells, an average density of 14.1 particles per source per cell would result from a monthly average sulfate concentration computation centered on one of our critical release points. If all particles were weighted equally, that particle density would be sufficient to avoid serious concentration estimation errors.

---

[3]That value is computed as follows: at each of 24 times of the day for each of (nominally) 30 days of the month, 48 particles are located in the horizontal plane (24 x 48 x 30 = 34560 particles per month). Because of the random number generators built into the model, each of these trajectory end points is unique.

However, each particle carries a magnitude which reflects its source's emission strength and diurnal cycle. That magnitude changes while in transit based on its probable chemical status and probable vertical dilution. Therefore we should be somewhat reserved about our judgement that enough particles have been defined. It seems reasonable to try a one hour time step with 2 mile by 2 mile (3.22 km by 3.22 km) receptor grid spacing, and then check to see that the computed results are free of serious defects.

5.3 Application of the Simulation Model to the Years 1972 through 1974

The air quality model described in Chapter 3 was programmed using the universal data handling package MAGIC maintained on the Caltech IBM 370/158 computer by R. C. Y. Koh. User supplied subroutines were constructed at those points in the program where computational efficiency is critical. These special routines cover trajectory integration, the model's pollutant chemistry, and particle counting in order to produce concentration estimates. A summary of program execution characteristics is given in Table 5.7.

In order to conserve computing resources, the model was instructed to compute source to receptor transport relationships only from source cells with noticeable emissions. If a source cell contributed less than 0.01 tons per day of SO_x emissions at the end of the source class aggregation process, the cell was treated as being vacant.

Model tests of the use of the one hour time step and 2 mile by 2 mile receptor cells revealed that the downwind sulfate concentration

TABLE 5.7

Execution Characteristics of
the Air Quality Simulation Model
Computer Program

Example Application: Computation of Sulfate Air Quality averaged over
the month of July 1974 at one value of the rate of SO_2
oxidation, k.

Input: (a) 845 virtual emissions sources divided among 11 source
             classes.

         (b) Meteorological data in time series for each hour of the
             month.

Output: (a) Sulfate concentration predictions within each of 625 receptor
             cells. It is required that air quality increments due to
             each source class be identified within each receptor cell.
             In effect that means that the model must repeat concentration
             calculations for each of eleven source classes.

         (b) Predicted values of the ratio of average sulfate to average
             total sulfur oxides concentrations within each of 625
             receptor cells.

         (c) Mass balance calculations on the fate of sulfur released.

         (d) Comparison of observed to predicted concentrations.

         (e) Fifteen contour or x-y plots.

Computational Characteristics of that Application:
         (a) Execution time: 25 minutes of CPU time on an IBM 370/158
             computer with MVS operating system.

         (b) Core storage used: 576 K bytes.

         (c) Direct cost at Caltech Computing Center including contour
             plots: $40.48 at low priority large-user discount rate;
             about $80 otherwise. Charges at other computing centers
             will vary according to accounting system.

         (d) Program utilizes some installation dependent features.

predictions were of acceptable quality. The concentration fields were generally free of spurious voids. Most features of the sulfate concentration patterns rise or fall in sequence across relative peaks and valleys which span the dimensions of several adjacent receptor cells.

The major drawback to the use of such a large time step occurs close to the source within the first hour of pollutant transport. An insufficient number of particles are present to define the shape of a plume with dimensions less than that of one of our receptor cells. To compound this problem, the assumption of instantaneous vertical mixing breaks down for some of those particles standing immediately above their release point from an elevated source at $(t-t_o)$ equals zero. For an illustration of that problem, see the early part of the plume in Case (1) of Figure 3.3.

Fortunately, this situation is easily resolved by one of a number of means. The first hour of pollutant transport is the only time period in the model in which unsteady meteorological conditions could be represented by a steady-state solution of the diffusion equation out to the distance of one time step downwind of the source. If we were interested mainly in concentrations of a primary contaminant from isolated low-level sources, that is the approach that would be taken. But because most observed sulfates are secondary pollutants formed by chemical reactions downwind of their source, highly accurate ground-level concentration estimates within the first few hundred meters from the stack are not as critical as they would be in many other

applications. If we resolve the singularity in the instantaneous

vertical mixing assumption at the source, most of our other problems

will vanish. That is because the definition of the shape of the plume

is not important to ground level pollutant concentrations if the plume

has not yet mixed to ground level.

Therefore, the following approach was adopted for this application

of the model within the existing framework of the model derivation.

The probabilities P_{SO_4} and P_{SO_2} that a pollutant particle contributes

to ground level air quality are set equal to zero for the case $\underset{\sim}{X} = \underset{\sim o}{X}$

and $t = t_o$ for all source classes, i, with elevated stack heights

$H(t_o,i)$. That merely says that a fresh pollutant particle just

released from an elevated source takes some non-zero time to mix to

ground level. In practice, particles of age $\tau = 0$ from stationary

source stacks will not be counted, while fresh emissions from ground-

level mobile sources will still contribute immediately to observed air

quality. This treatment was tested within the context of several

monthly simulations. It was found to perform well enough that other

corrective actions such as decreasing the time step, altering the

receptor cell size or replacing the first hour of transport by an

analytical solution to the diffusion equation will be deferred until

an application arises which requires such attention.

The air quality model was applied to the task of predicting

sulfate concentrations within the relatively level portion of the Los

Angeles Basin and the San Gabriel Valley. That receptor zone is

identical to our emissions grid of Figure 4.7, less the San Fernando

Valley (squares I 1-10 by J 20-25). Receptor zone selection was discussed in Chapters 2 and 3 on the basis of terrain considerations, coverage of air monitoring stations and inclusion of major source locations.

Convergence to a final estimate of the value of the rate constant, k, within the tolerance limits previously described (see footnote 2, section 5.2 of this chapter) was attained within an average of 2.25 iterations per month. An initial trial value of k for each month was obtained by scanning the measured values of f_s appearing in various months of the year in relation to values of f_s observed during July 1973, the month for which we had measured values for k. A subsequent selection of k for a second iteration on each month was usually necessary. That process was aided by evaluating the following linearized expression at each air monitoring site.

$$\frac{k_{new}}{k_{old}} \approx \frac{\overline{<c_{SO_4}>}_{observed} - \overline{<c_{SO_4}>}_{background}}{\overline{<c_{SO_4}>}_{predicted} - \overline{<c_{SO_4}>}_{background}} \qquad (5.6)$$

where

k_{old} is the value of k from the most recent iteration.

k_{new} is the next guess for an improved value of k.

$\overline{<c_{SO_4}>}_{observed}$ is average sulfate concentration measured at that air monitoring station for the month of interest.

$\overline{<c_{SO_4}>}_{predicted}$ is the average sulfate concentration predicted at that monitoring site at the last model iteration.

$\overline{<c_{SO_4}>}_{background}$ is that month's average background sulfate concentration estimate.

These values of k_{new} from ten to eleven monitoring sites in each month were usually averaged and then rounded to the nearest whole percent per hour, or appropriate fraction thereof in accordance with our tolerance limits on k. The iteration procedure would stop when all values of k_{new} were within the same tolerance limit interval on k_{old}, or when a value of k is attained which was straddled by groups of monitoring sites demanding that iterations proceed in opposing directions. This latter circumstance can occur even when all values of $\overline{<c_{SO_4}>}_{predicted}$ are within the error bounds on $\overline{<c_{SO_4}>}_{observed}$. That is because values of $\overline{<c_{SO_4}>}_{observed}$ are known only to within large error bounds at some stations in some months.

5.4 Air Quality Model Results

5.4.1 Predicted Versus Observed Sulfate Concentrations

Figures 5.6(a) through 5.16(a) present the results of the air quality simulation model in time series at each of the LAAPCD and CHESS air monitoring stations located within our receptor zone. Model results are represented by a horizontal solid line which rises and falls in the form of a bar graph. The open symbols represent the arithmetic mean of all sulfate measurements at each monitoring site in each month. The error bounds shown reflect 95% confidence intervals on the mean value of the air quality observations (see Appendix B4). Any model

MONTHLY ARITHMETIC MEAN SULFATE CONCENTRATIONS AT DOWNTOWN LOS ANGELES (APCD)

AIR QUALITY MODEL RESULTS VS. OBSERVED VALUES
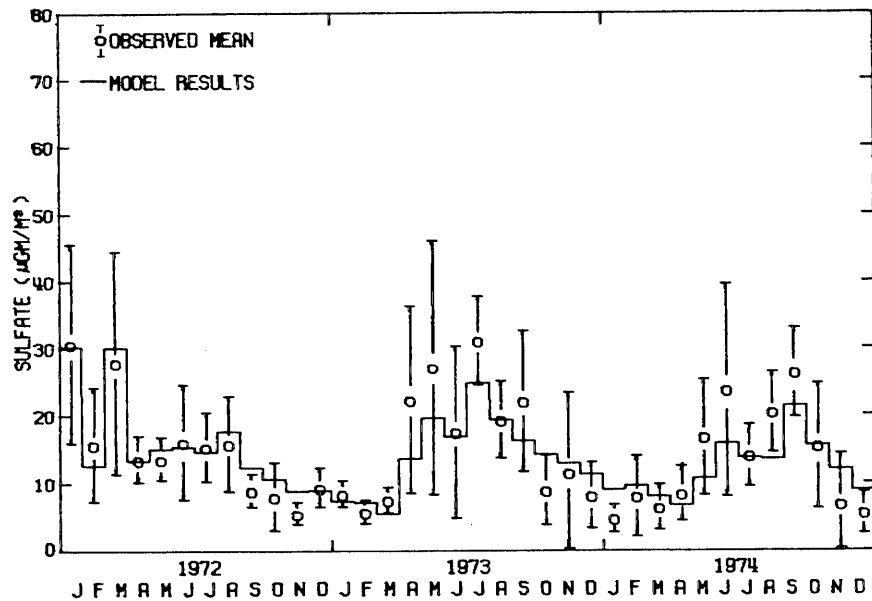
FIGURE 5.6(a)

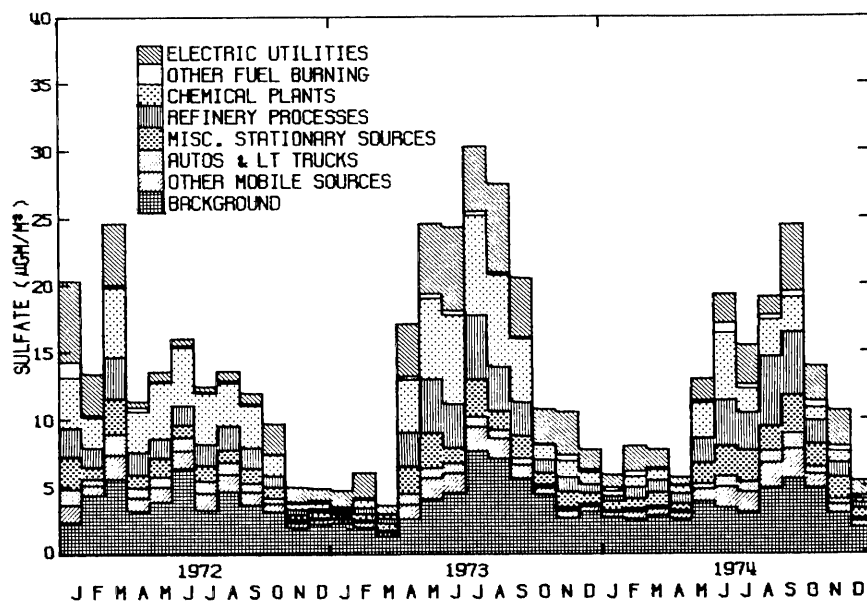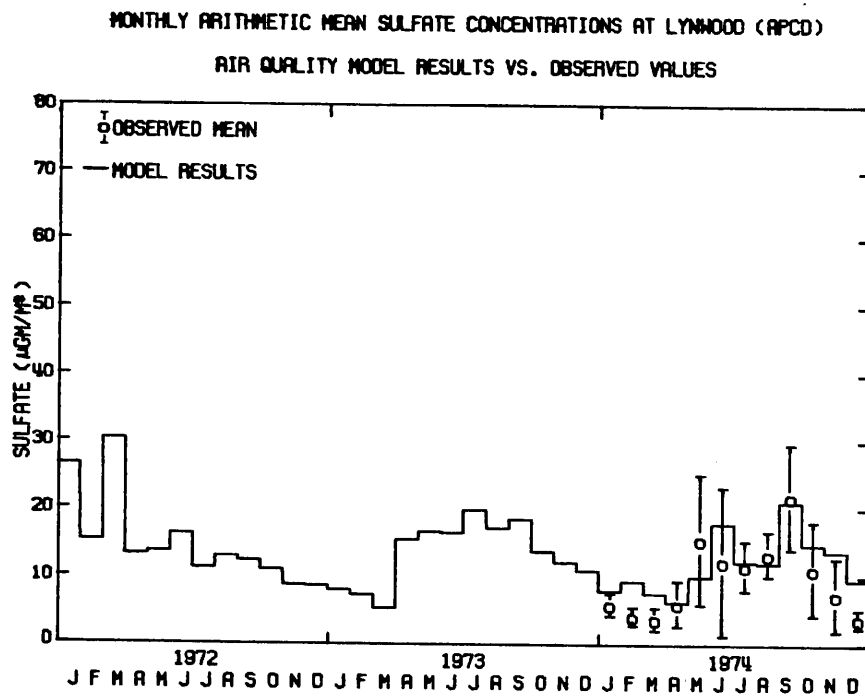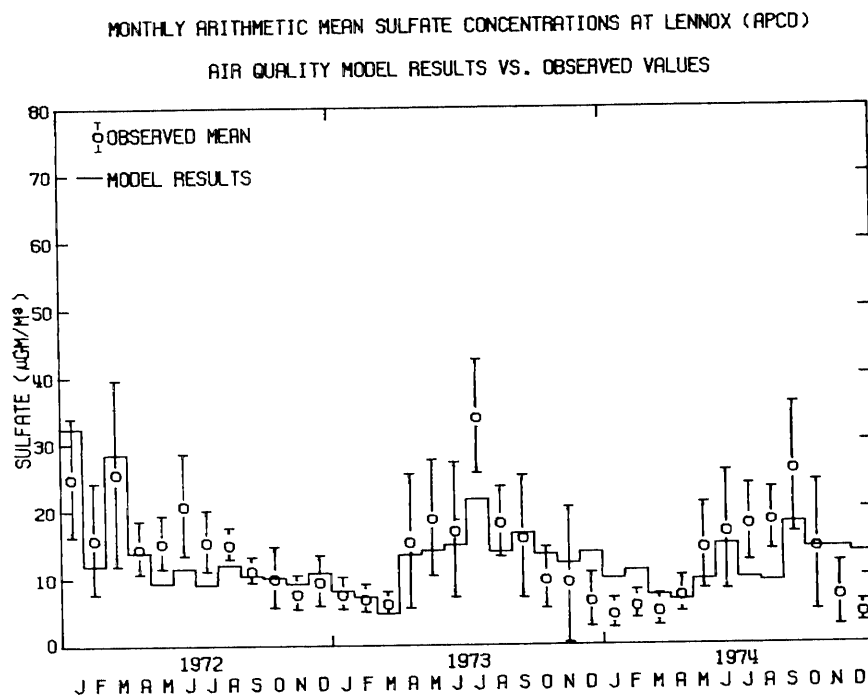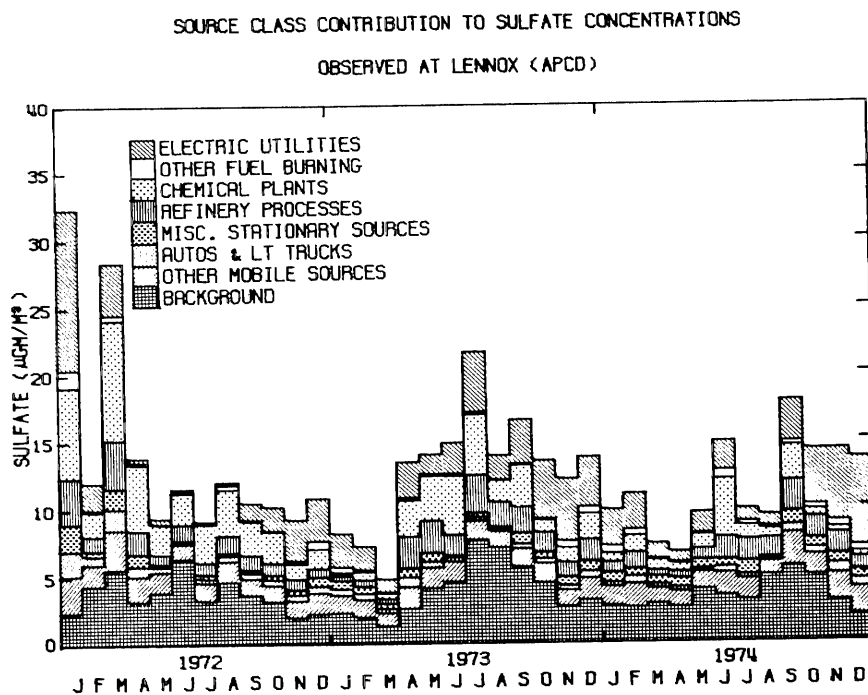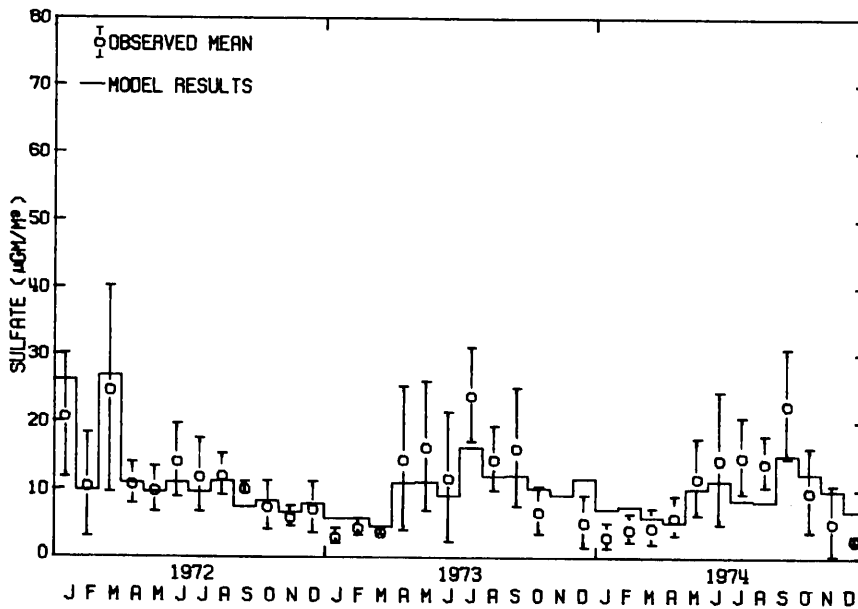SOURCE CLASS CONTRIBUTION TO SULFATE CONCENTRATIONS
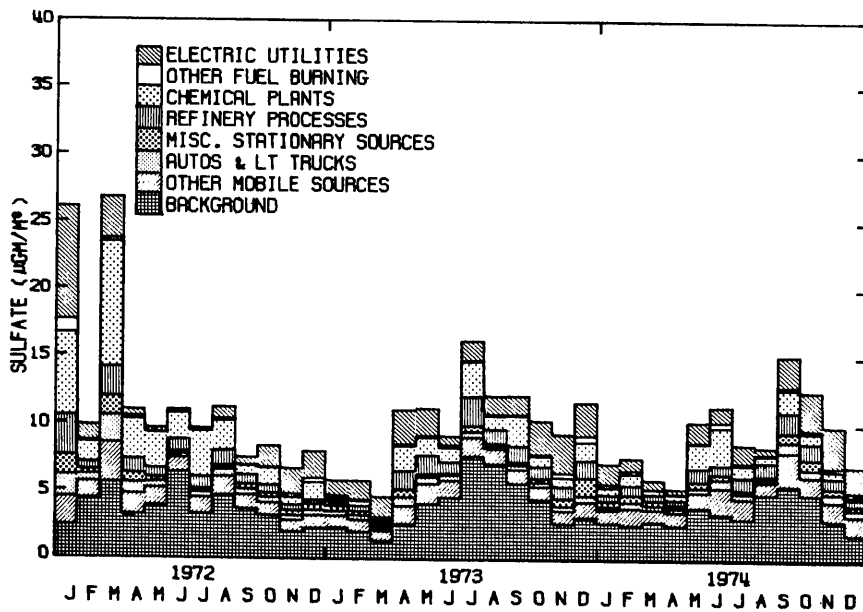
OBSERVED AT DOWNTOWN LOS ANGELES (APCD)
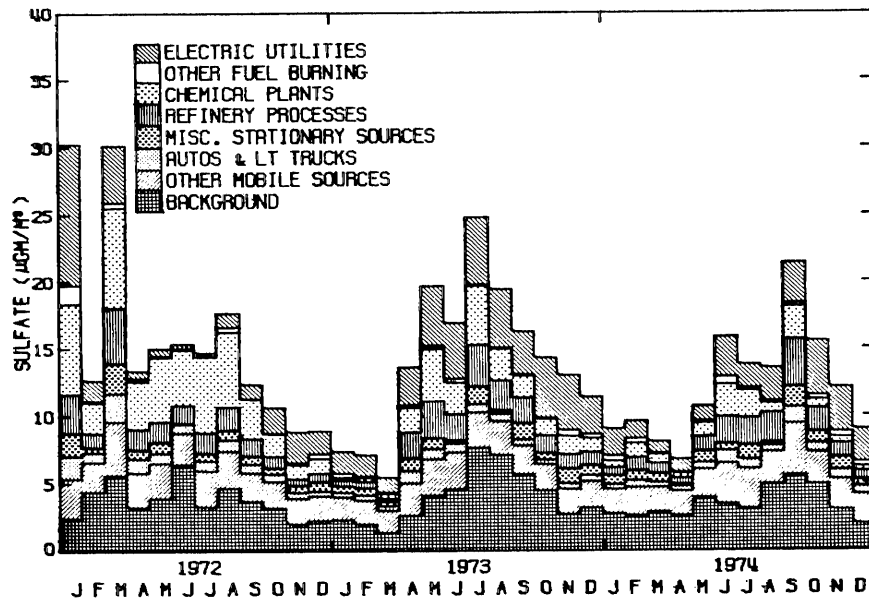
FIGURE 5.6(b)

MONTHLY ARITHMETIC MEAN SULFATE CONCENTRATIONS AT PASADENA (APCD)
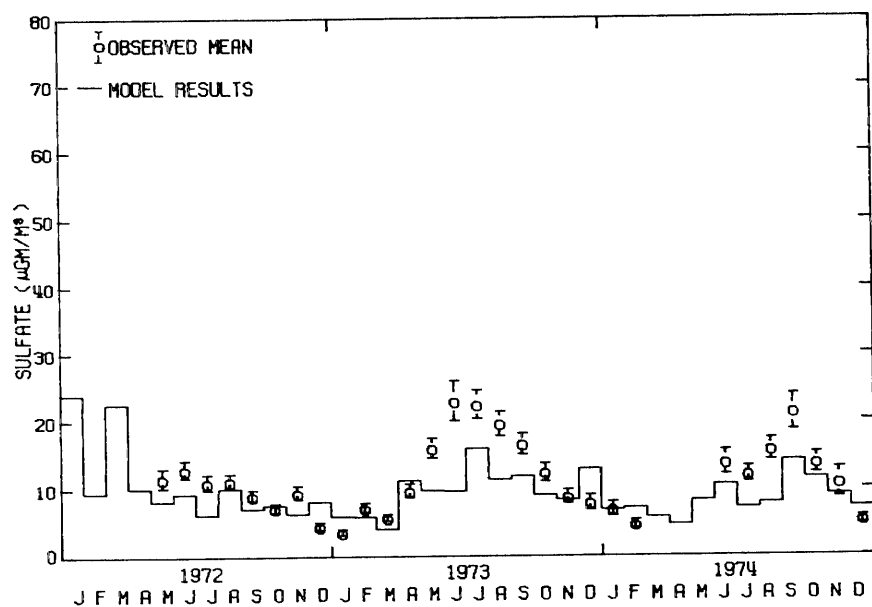
AIR QUALITY MODEL RESULTS VS. OBSERVED VALUES
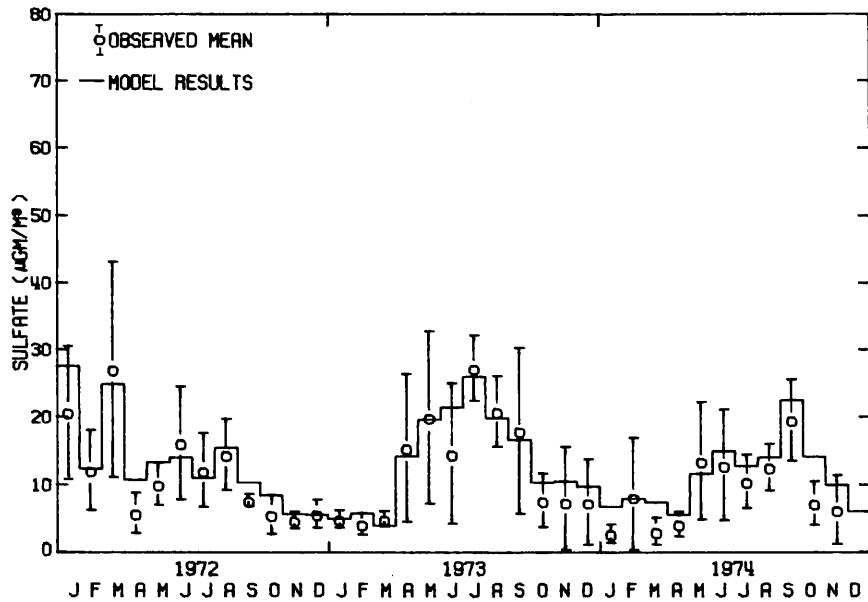
FIGURE 5.7(a)

SOURCE CLASS CONTRIBUTION TO SULFATE CONCENTRATIONS

OBSERVED AT PASADENA (APCD)
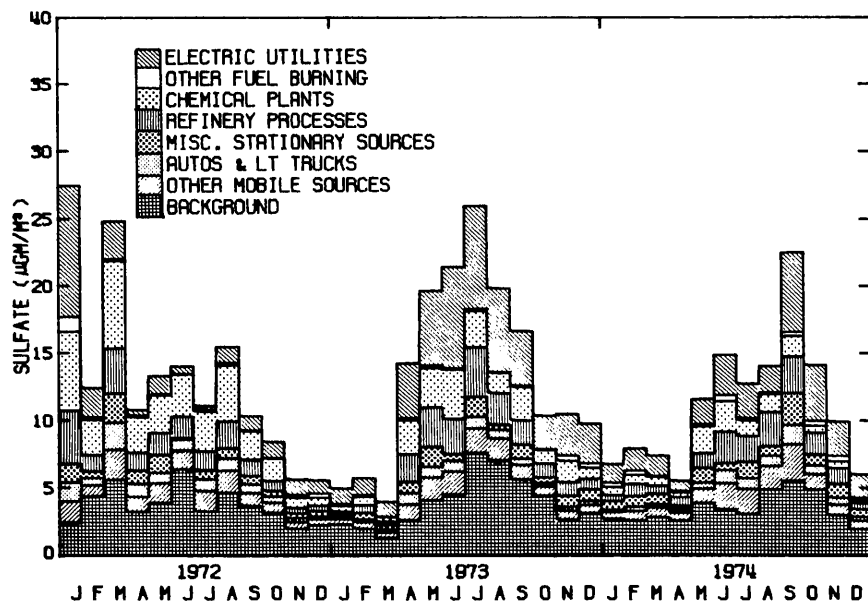
FIGURE 5.7(b)

MONTHLY ARITHMETIC MEAN SULFATE CONCENTRATIONS AT AZUSA (APCD)

AIR QUALITY MODEL RESULTS VS. OBSERVED VALUES
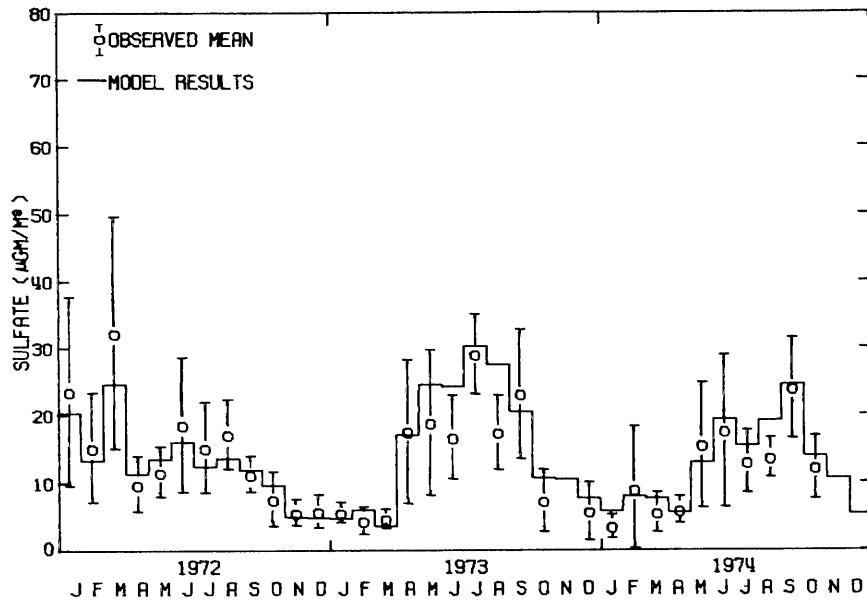
FIGURE 5.8(a)

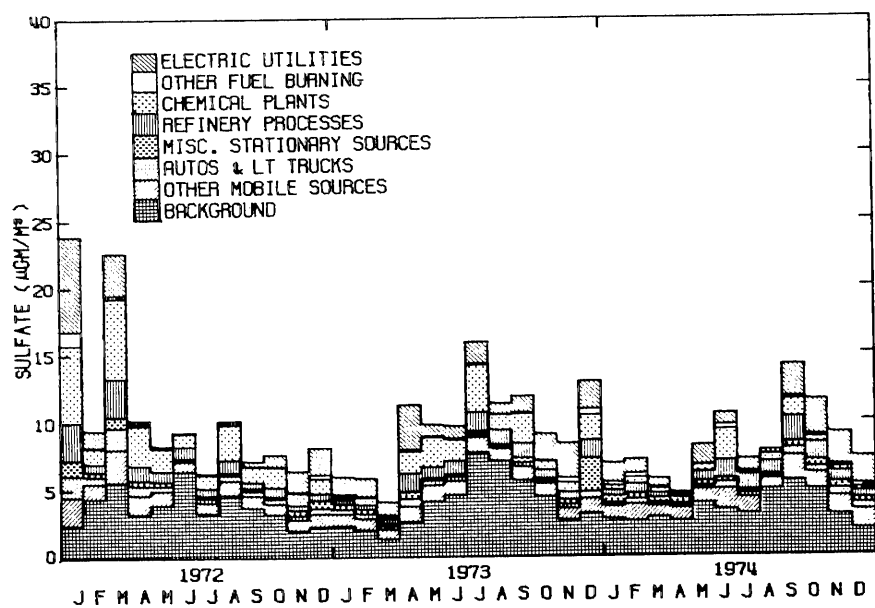SOURCE CLASS CONTRIBUTION TO SULFATE CONCENTRATIONS

OBSERVED AT AZUSA (APCD)

FIGURE 5.8(b)

299

MONTHLY ARITHMETIC MEAN SULFATE CONCENTRATIONS AT LYNWOOD (APCD)
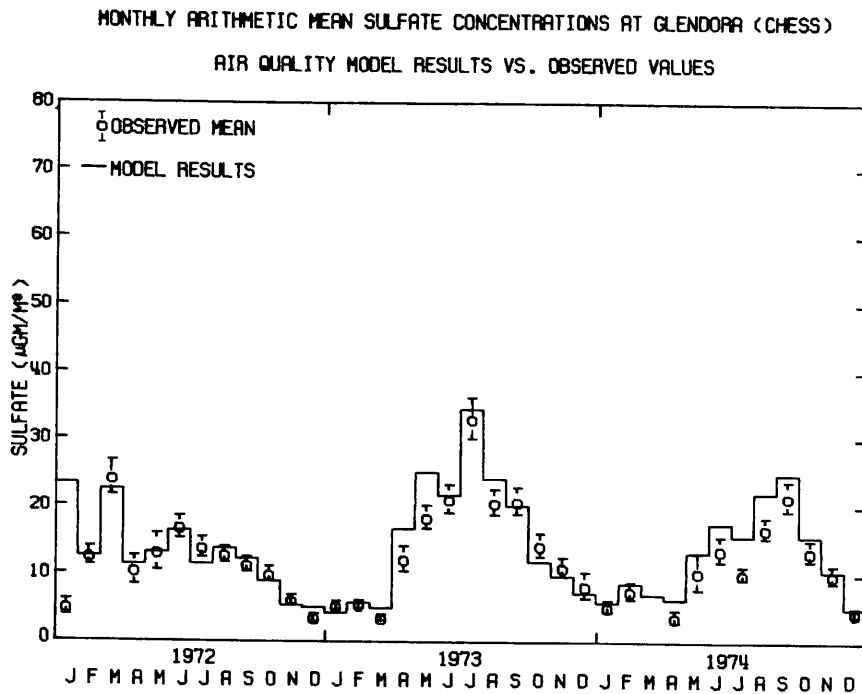
AIR QUALITY MODEL RESULTS VS. OBSERVED VALUES

FIGURE 5.9(a)

SOURCE CLASS CONTRIBUTION TO SULFATE CONCENTRATIONS
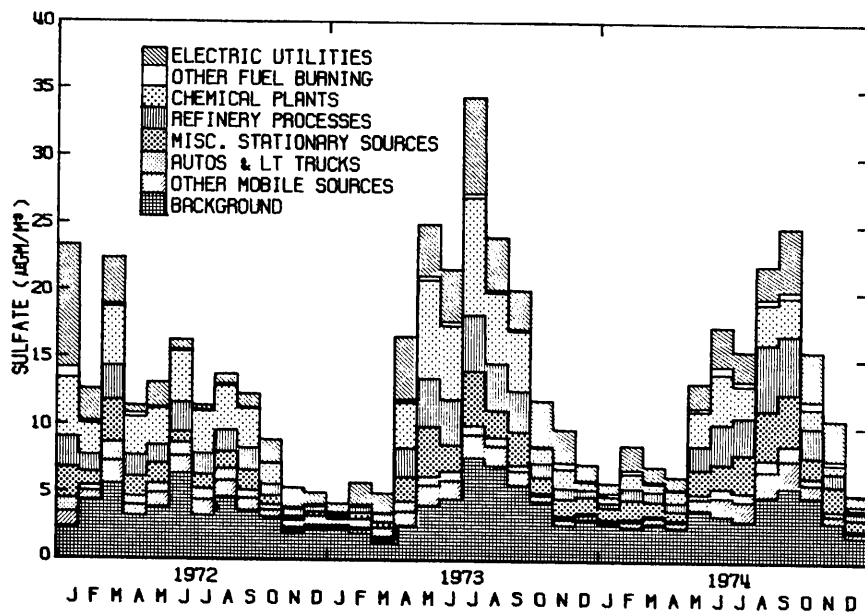
OBSERVED AT LYNWOOD (APCD)

FIGURE 5.9(b)

300

MONTHLY ARITHMETIC MEAN SULFATE CONCENTRATIONS AT LENNOX (APCD)

AIR QUALITY MODEL RESULTS VS. OBSERVED VALUES

FIGURE 5.10(a)

SOURCE CLASS CONTRIBUTION TO SULFATE CONCENTRATIONS

OBSERVED AT LENNOX (APCD)
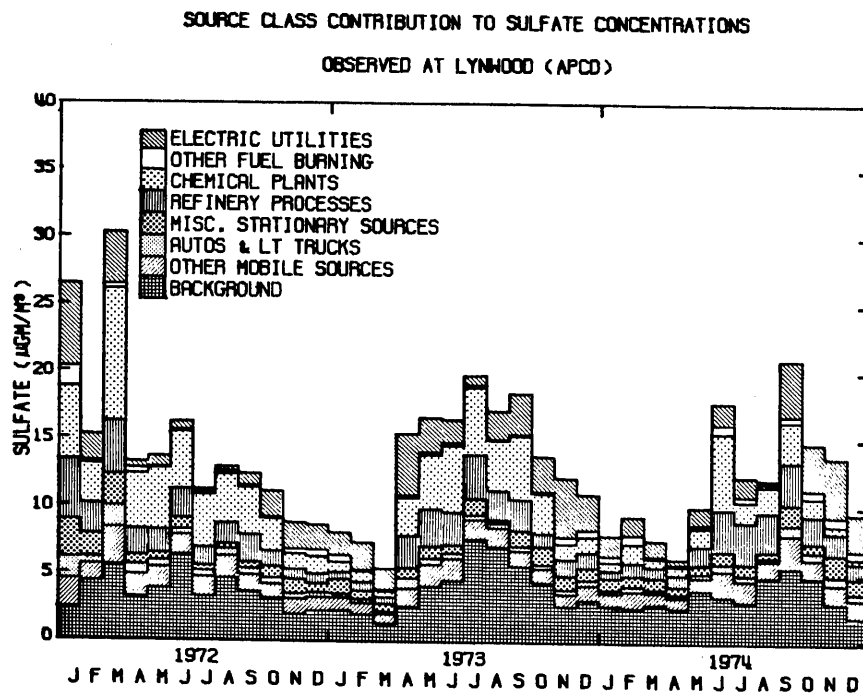
FIGURE 5.10(b)

MONTHLY ARITHMETIC MEAN SULFATE CONCENTRATIONS AT WEST LOS ANGELES (APCD)

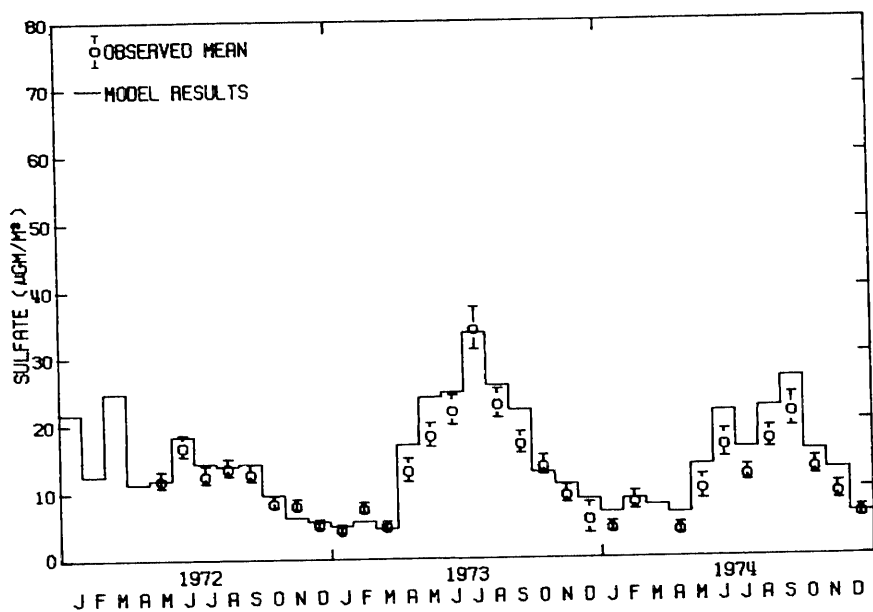AIR QUALITY MODEL RESULTS VS. OBSERVED VALUES

FIGURE 5.11(a)

SOURCE CLASS CONTRIBUTION TO SULFATE CONCENTRATIONS

OBSERVED AT WEST LOS ANGELES (APCD)

FIGURE 5.11(b)

MONTHLY ARITHMETIC MEAN SULFATE CONCENTRATIONS AT SANTA MONICA (CHESS)

AIR QUALITY MODEL RESULTS VS. OBSERVED VALUES

FIGURE 5.12(a)

SOURCE CLASS CONTRIBUTION TO SULFATE CONCENTRATIONS
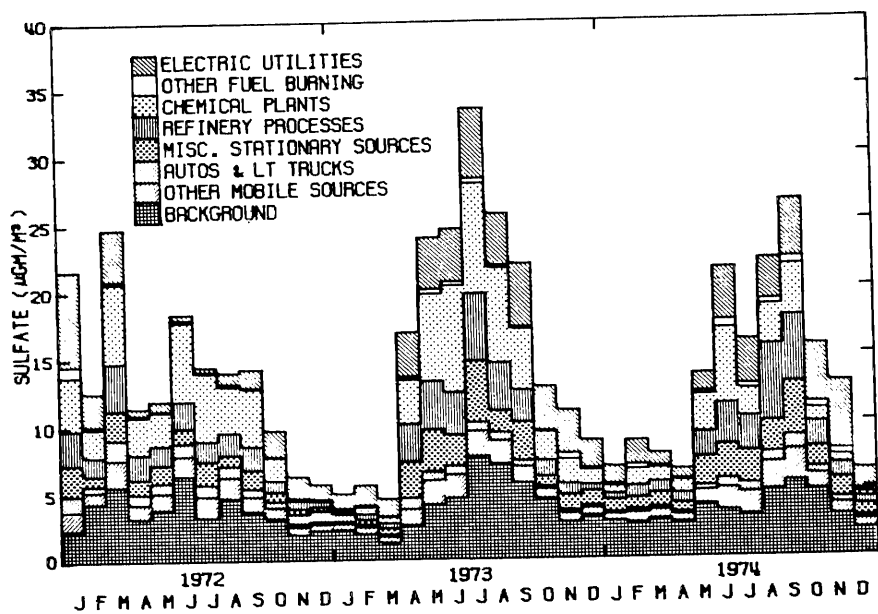
OBSERVED AT SANTA MONICA (CHESS)

FIGURE 5.12(b)

MONTHLY ARITHMETIC MEAN SULFATE CONCENTRATIONS AT GLENDORA (CHESS)

AIR QUALITY MODEL RESULTS VS. OBSERVED VALUES

FIGURE 5.13(a)

SOURCE CLASS CONTRIBUTION TO SULFATE CONCENTRATIONS

OBSERVED AT GLENDORA (CHESS)

FIGURE 5.13(b)

MONTHLY ARITHMETIC MEAN SULFATE CONCENTRATIONS AT WEST COVINA (CHESS)

AIR QUALITY MODEL RESULTS VS. OBSERVED VALUES

FIGURE 5.14(a)

SOURCE CLASS CONTRIBUTION TO SULFATE CONCENTRATIONS

OBSERVED AT WEST COVINA (CHESS)

FIGURE 5.14(b)

305

MONTHLY ARITHMETIC MEAN SULFATE CONCENTRATIONS AT GARDEN GROVE (CHESS)
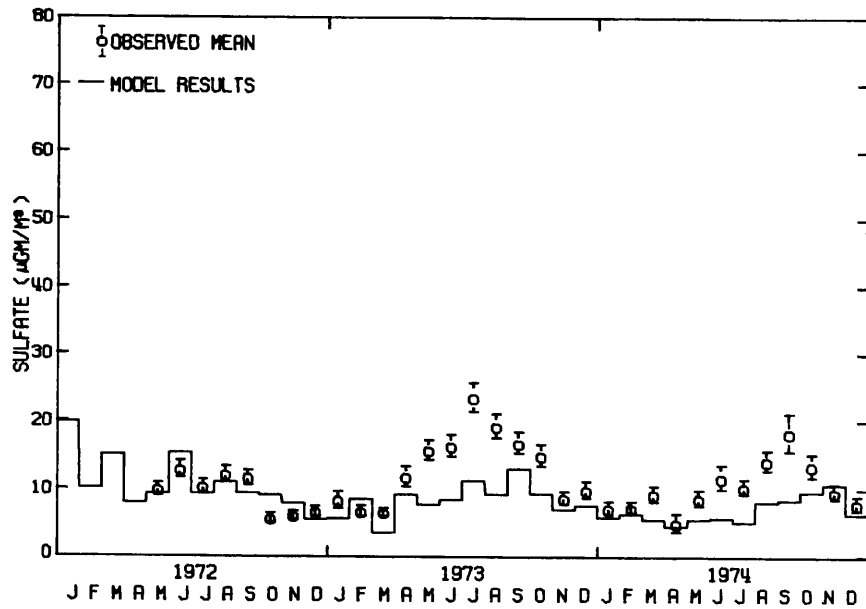
AIR QUALITY MODEL RESULTS VS. OBSERVED VALUES

FIGURE 5.15(a)

SOURCE CLASS CONTRIBUTION TO SULFATE CONCENTRATIONS

OBSERVED AT GARDEN GROVE (CHESS)

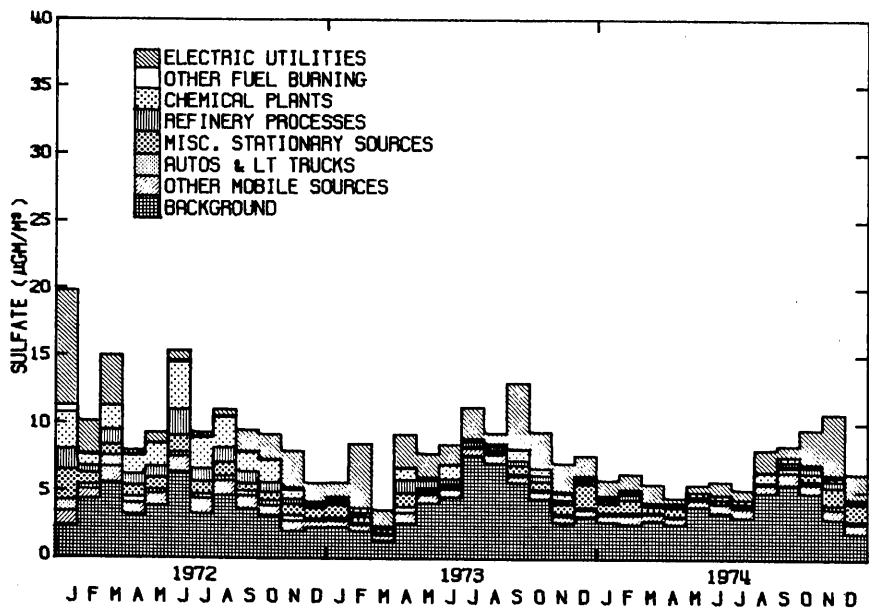FIGURE 5.15(b)

306

MONTHLY ARITHMETIC MEAN SULFATE CONCENTRATIONS AT ANAHEIM (CHESS)
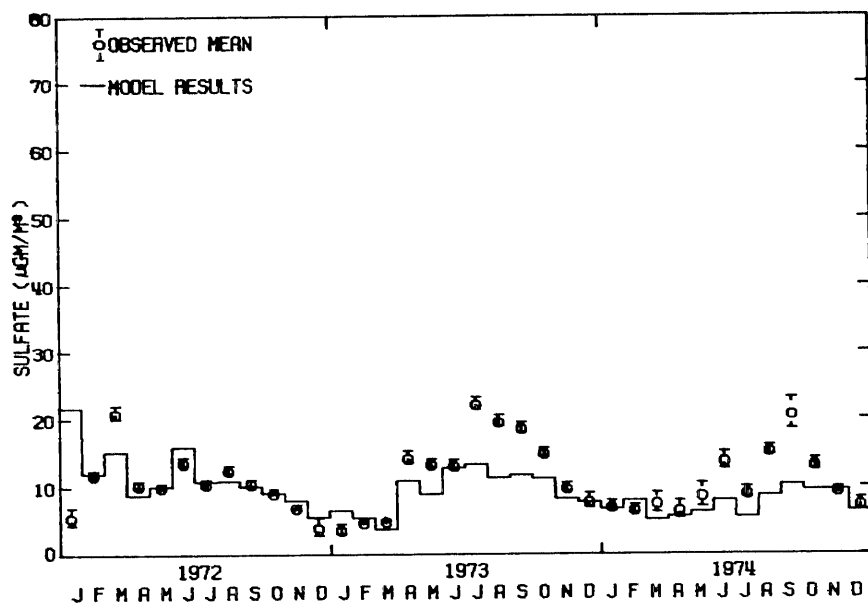
AIR QUALITY MODEL RESULTS VS. OBSERVED VALUES

FIGURE 5.16(a)

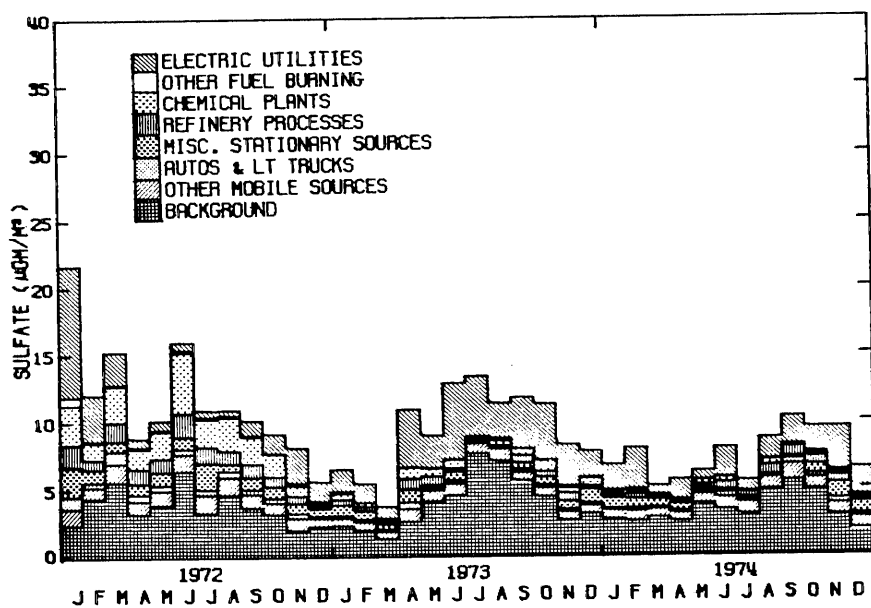SOURCE CLASS CONTRIBUTION TO SULFATE CONCENTRATIONS

OBSERVED AT ANAHEIM (CHESS)

FIGURE 5.16(b)

prediction which threads those error bounds is indistinguishable from the field measurements.[4]

Approximately eighty percent of the sulfate concentration predictions at the LAAPCD stations are within the error bounds on the ambient monitoring results. At the CHESS stations the error bounds on the ambient data are much tighter due to the increased sampling schedule, and fewer predictions fall within the error bounds on the field observations. Model predictions still track observed sulfate levels closely at the critical CHESS stations in the Eastern San Gabriel Valley at Glendora and West Covina. A tendency to underpredict the summer peaks observed near the up-coast and down-coast edges of our receptor area at Santa Monica and at Garden Grove and Anaheim during 1973 and 1974 is noted.

Monthly concentration predictions can be pooled to form annual arithmetic mean sulfate estimates throughout the airshed. These annual average sulfate concentration predictions can be compared to observations at a larger number of air monitoring stations, as shown in Tables 5.8, 5.9 and 5.10. Sixty-four percent of the annual mean sulfate concentration predictions which can be compared to air quality

---

[4]An assessment of air quality model results against the criterion that they be indistinguishable from the ambient monitoring data is both the most severe and also the most appropriate test of model performance that this author has encountered. Most air quality model validation studies compare the correlation between observations and predictions or some measure of the ratio of observed to predicted air quality levels. Some of these more customary statistical measures of model performance will be presented shortly.

308

TABLE 5.8

OBSERVED VERSUS PREDICTED ANNUAL AVERAGE SULFATE AIR QUALITY
FOR THE YEAR 1972

(CONCENTRATIONS STATED IN $\mu GM/M^3$ AS $SO_4^=$)

		SULFATE AIR QUALITY OBSERVATIONS					SULFATE AIR QUALITY MODEL RESULTS		
		SAMPLE ARITHMETIC MEAN $\bar{y}$	SAMPLE ARITHMETIC STANDARD DEVIATION σ	NUMBER OF DAYS SAMPLED n	LOWER CONFIDENCE LIMIT ON $\bar{y}$ (2.5 %ile)	UPPER CONFIDENCE LIMIT ON $\bar{y}$ (97.5 %ile)	ARITHMETIC MEAN FROM AIR QUALITY MODEL	PREDICTION IS WITHIN CONFIDENCE INTERVAL ON OBSERVATIONS	DIFFERENCE BETWEEN OBSERVED AND PREDICTED MEANS
SANTA MONICA	CHESS	9.40	5.84	238.00	8.87	9.92	10.82	NOTE (b)	NOTE (b)
WEST LA	LAAPCD	11.86	9.04	72.00	9.98	13.74	12.20	YES	-0.34
LENNOX	LAAPCD	15.37	9.78	73.00	13.35	17.39	14.16	YES	1.21
TORRANCE	NASN	11.34	6.35	30.00	9.15	13.52	13.81	NO	-2.47
LONG BEACH	NASN	11.29	7.55	28.00	8.59	13.98	15.06	NO	-3.77
LYNWOOD	LAAPCD	*	*	0.0	*	*	15.05	NOTE (a)	NOTE (a)
GLENDALE	NASN	10.27	7.27	28.00	7.68	12.87	12.39	YES	-2.12
LOS ANGELES	NASN	11.07	8.19	32.00	8.35	13.79	15.88	NO	-4.81
LOS ANGELES	LAAPCD	14.38	11.60	68.00	11.88	16.88	15.88	YES	-1.50
PASADENA	LAAPCD	11.55	10.77	70.00	9.27	13.82	13.32	YES	-1.77
PASADENA	NASN	10.67	7.58	27.00	7.91	13.43	13.32	YES	-2.65
GARDEN GROVE	CHESS	9.20	5.39	239.00	8.72	9.69	10.86	NOTE (b)	NOTE (b)
ANAHEIM	CHESS	10.95	7.68	328.00	10.52	11.39	11.57	NOTE (b)	NOTE (b)
ANAHEIM	NASN	11.19	8.24	28.00	8.25	14.13	11.57	YES	-0.38
SANTA ANA	NASN	11.69	11.06	29.00	7.82	15.56	9.56	YES	2.13
AZUSA	LAAPCD	13.98	11.91	71.00	11.48	16.48	13.09	YES	0.89
WEST COVINA	CHESS	11.06	6.77	241.00	10.46	11.66	13.57	NOTE (b)	NOTE (b)
GLENDORA	CHESS	11.98	9.63	303.00	11.38	12.58	13.02	NOTE (b)	NOTE (b)

NOTES: (a) AN ASTERISK (*) INDICATES DATA THAT ARE UNAVAILABLE.

(b) ANNUAL MEANS CALCULATED AT THESE AIR MONITORING SITES ARE BIASED BEYOND THE ASSUMPTIONS OF THE CONFIDENCE INTERVAL CALCULATIONS. SAMPLING AT SANTA MONICA, GARDEN GROVE AND WEST COVINA DID NOT BEGIN UNTIL MAY 1972. SAMPLING AT ANAHEIM AND GLENDORA DID NOT BEGIN UNTIL THE LAST FEW DAYS OF JANUARY 1972. ALL CHESS MONITORING SITES WERE OUT OF OPERATION DURING THE EARLY JANUARY 1972 SULFATE EPISODES, AND MOST CHESS STATIONS MISSED THE MARCH 1972 SULFATE EPISODES AS WELL.

TABLE 5.9

OBSERVED VERSUS PREDICTED ANNUAL AVERAGE SULFATE AIR QUALITY
FOR THE YEAR 1973

(CONCENTRATIONS STATED IN $\mu GM/M^3$ AS $SO_4^=$)

		SULFATE AIR QUALITY OBSERVATIONS					SULFATE AIR QUALITY MODEL RESULTS		
		SAMPLE ARITHMETIC MEAN ȳ	SAMPLE ARITHMETIC STANDARD DEVIATION σ	NUMBER OF DAYS SAMPLED n	LOWER CONFIDENCE LIMIT ON ȳ (2.5 %ile)	UPPER CONFIDENCE LIMIT ON ȳ (97.5 %ile)	ARITHMETIC MEAN FROM AIR QUALITY MODEL	PREDICTION IS WITHIN CONFIDENCE INTERVAL ON OBSERVATIONS	DIFFERENCE BETWEEN OBSERVED AND PREDICTED MEANS
SANTA MONICA	CHESS	12.49	10.10	354.00	12.04	12.94	9.71	NO	2.78
WEST LA	LAAPCD	10.63	10.47	71.00	8.44	12.83	9.96	YES	0.67
LENNOX	LAAPCD	13.94	12.17	73.00	11.43	16.45	12.87	YES	1.07
TORRANCE	NASN	11.21	7.43	25.00	8.39	14.03	12.16	YES	-0.95
LONG BEACH	NASN	10.59	5.58	25.00	8.47	12.70	13.65	NO	-3.06
LYNWOOD	LAAPCD	*	*	0.0	*	*	13.49	NOTE (a)	NOTE (a)
GLENDALE	NASN	10.46	7.82	30.00	7.77	13.15	10.55	YES	-0.09
LOS ANGELES	NASN	12.30	6.59	25.00	9.80	14.80	14.14	YES	-1.84
LOS ANGELES	LAAPCD	15.80	14.70	73.00	12.77	18.83	14.14	YES	-1.66
PASADENA	LAAPCD	12.66	12.33	73.00	10.12	15.20	13.65	YES	-0.99
PASADENA	NASN	13.59	9.93	30.00	10.18	17.00	13.65	YES	-0.06
GARDEN GROVE	CHESS	13.23	8.76	352.00	12.79	13.67	8.39	NO	4.84
ANAHEIM	CHESS	12.31	9.18	352.00	11.88	12.75	9.37	NO	2.94
ANAHEIM	NASN	9.48	5.40	25.00	7.43	11.54	9.37	YES	0.11
SANTA ANA	NASN	8.02	3.64	25.00	6.64	9.41	7.98	YES	0.04
AZUSA	LAAPCD	13.11	11.98	73.00	10.64	15.58	15.72	NO	-2.61
WEST COVINA	CHESS	14.54	12.00	347.00	13.98	15.09	16.26	NO	-1.72
GLENDORA	CHESS	14.43	12.10	356.00	13.91	14.95	15.53	NO	-1.10

NOTE: (a) AN ASTERISK (*) INDICATES DATA THAT ARE UNAVAILABLE.

TABLE 5.10

OBSERVED VERSUS PREDICTED ANNUAL AVERAGE SULFATE AIR QUALITY
FOR THE YEAR 1974

(CONCENTRATIONS STATED IN $\mu GM/M^3$ AS $SO_4^=$)

		SULFATE AIR QUALITY OBSERVATIONS					SULFATE AIR QUALITY MODEL RESULTS		
		SAMPLE ARITHMETIC MEAN $\bar{y}$	SAMPLE ARITHMETIC STANDARD DEVIATION σ	NUMBER OF DAYS SAMPLED n	LOWER CONFIDENCE LIMIT ON y (2.5 %ile)	UPPER CONFIDENCE LIMIT ON y (97.5 %ile)	ARITHMETIC MEAN FROM AIR QUALITY MODEL	PREDICTION IS WITHIN CONFIDENCE INTERVAL ON OBSERVATIONS	DIFFERENCE BETWEEN OBSERVED AND PREDICTED MEANS
SANTA MONICA	CHESS	11.32	8.95	248.00	10.59	12.05	8.35	NOTE (b)	NOTE (b)
WEST LA	LAAPCD	9.42	8.92	72.00	7.57	11.28	9.08	YES	0.34
LENNOX	LAAPCD	11.82	10.01	73.00	9.76	13.89	11.53	YES	0.29
TORRANCE	NASN	11.65	6.29	28.00	9.40	13.89	11.24	YES	0.41
LONG BEACH	NASN	13.95	9.21	26.00	10.53	17.37	12.24	YES	1.71
LYNWOOD	LAAPCD	9.47	8.55	68.00	7.63	11.31	11.86	NO	-2.39
GLENDALE	NASN	9.02	8.80	13.00	4.31	13.72	9.40	YES	-0.38
LOS ANGELES	NASN	13.92	12.09	26.00	9.43	18.41	12.12	YES	1.80
LOS ANGELES	LAAPCD	12.66	11.19	71.00	10.31	15.00	12.12	YES	0.54
PASADENA	LAAPCD	8.56	8.41	71.00	6.80	10.32	11.15	NO	-2.59
PASADENA	NASN	11.47	9.23	22.00	7.72	15.22	11.15	YES	0.32
GARDEN GROVE	CHESS	10.09	6.82	307.00	9.65	10.52	6.82	NO	3.27
ANAHEIM	CHESS	10.69	7.89	286.00	10.15	11.24	7.51	NO	3.18
ANAHEIM	NASN	12.51	9.10	30.00	9.38	15.63	7.51	NO	5.00
SANTA ANA	NASN	11.47	7.48	29.00	8.85	14.09	6.83	NO	4.64
AZUSA	LAAPCD	10.54	9.96	71.00	8.45	12.62	12.41	YES	1.87
WEST COVINA	CHESS	11.49	9.00	293.00	10.90	12.09	13.73	NOTE (b)	NOTE (b)
GLENDORA	CHESS	11.13	9.08	278.00	10.49	11.77	12.72	NOTE (b)	NOTE (b)

NOTE: (b) ANNUAL MEANS CALCULATED FROM OBSERVATIONS AT THESE AIR MONITORING SITES ARE BIASED BEYOND THE ASSUMPTIONS OF THE CONFIDENCE INTERVAL CALCULATIONS. THE CHESS STATION AT SANTA MONICA DID NOT FUNCTION DURING THE MONTHS OF MARCH, APRIL AND MAY, 1974. OBSERVATIONS AT WEST COVINA AND GLENDORA ARE ABSENT DURING MARCH 1974, AND ARE INFREQUENT DURING APRIL AND MAY. ANAHEIM AND GARDEN GROVE CHESS STATIONS SHOW ACTIVITY IN ALL MONTHS, BUT SAMPLING RATE FALLS DURING THE SAME PERIOD OF TIME.

measurements fall within the 95% confidence intervals on the sulfate

air quality measurements.

5.4.2 The Spatial-Temporal Correlation between Observed and Predicted
       Sulfate Concentrations

Figures 5.17 through 5.19 show the correspondence between

observed and predicted sulfate concentrations at all CHESS and LAAPCD

stations for all months with useful observations within each of the

years 1972, 1973 and 1974. A summary of the statistics of those data

sets is given in Table 5.11. Model performance is particularly good

during 1972 and 1973, and is felt to be acceptable during 1974.

The correlation between observed and predicted sulfate levels is

0.82 in both 1972 and 1973. From a visual comparison of Figures 5.17

and 5.18, most observers would hold that the 1972 model results

represent a far better fit to the observations than was obtained in

1973. The statistics of the 1972 data set are degraded by two outlying

data points with sulfate predictions of about 20 $\mu gm/m^3$ and observed

values near 5 $\mu gm/m^3$. Those two data points were examined more closely.

It was found that they are an artifact of the start-up of the CHESS

air monitoring network. The CHESS air monitoring stations at Anaheim

and Glendora initiated sampling during the closing days of January

1972. They thus missed sampling the high sulfate episodes which

occurred earlier in that month. With those two observations discarded

as biased, the remaining data for 1972 show a 0.89 correlation between

observations and model predictions.

SULFATE AIR QUALITY MODEL RESULTS – 1972

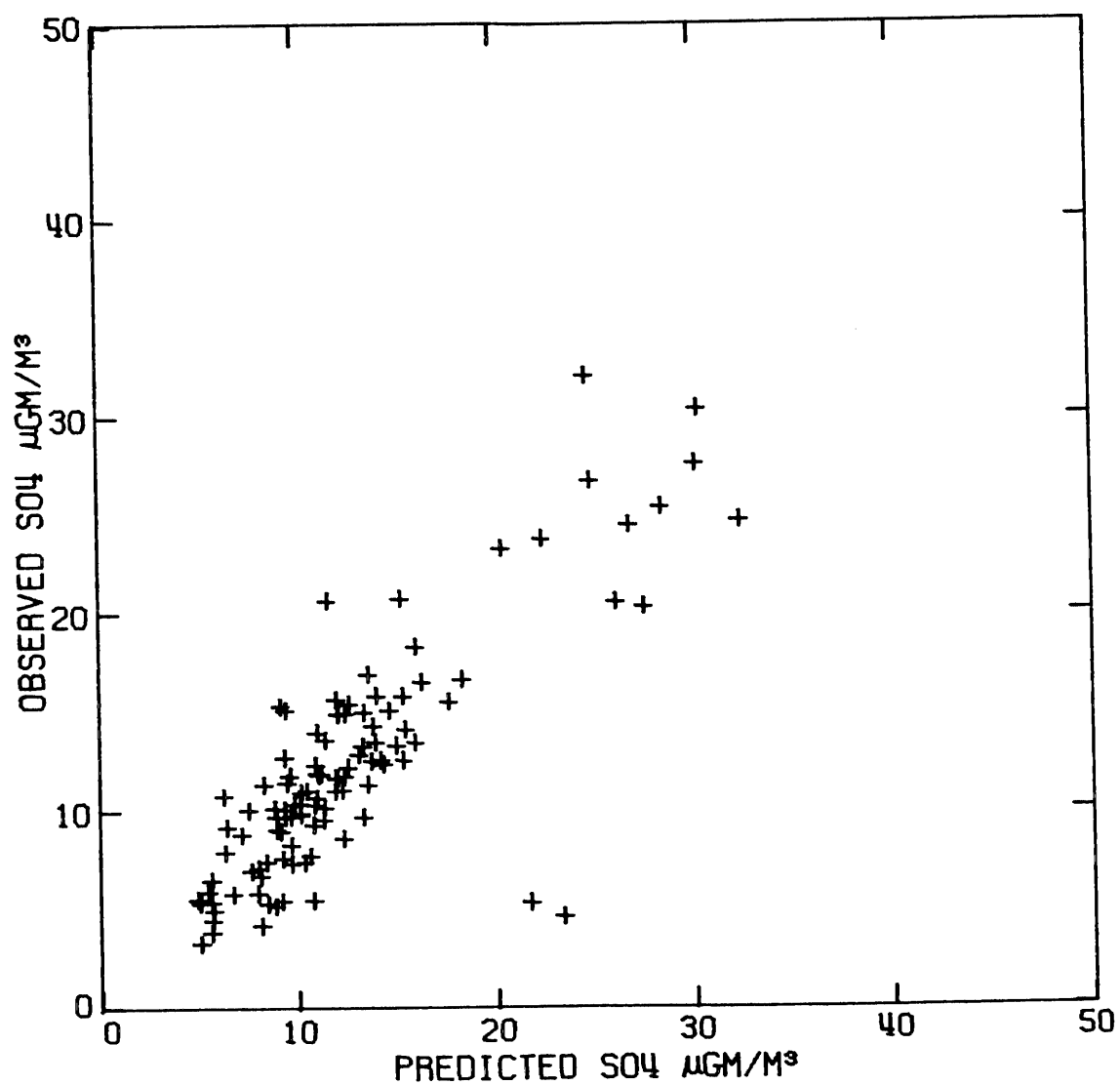MONTHLY MEANS AT TEN AIR MONITORING STATIONS

FIGURE 5.17

SULFATE AIR QUALITY MODEL RESULTS – 1973
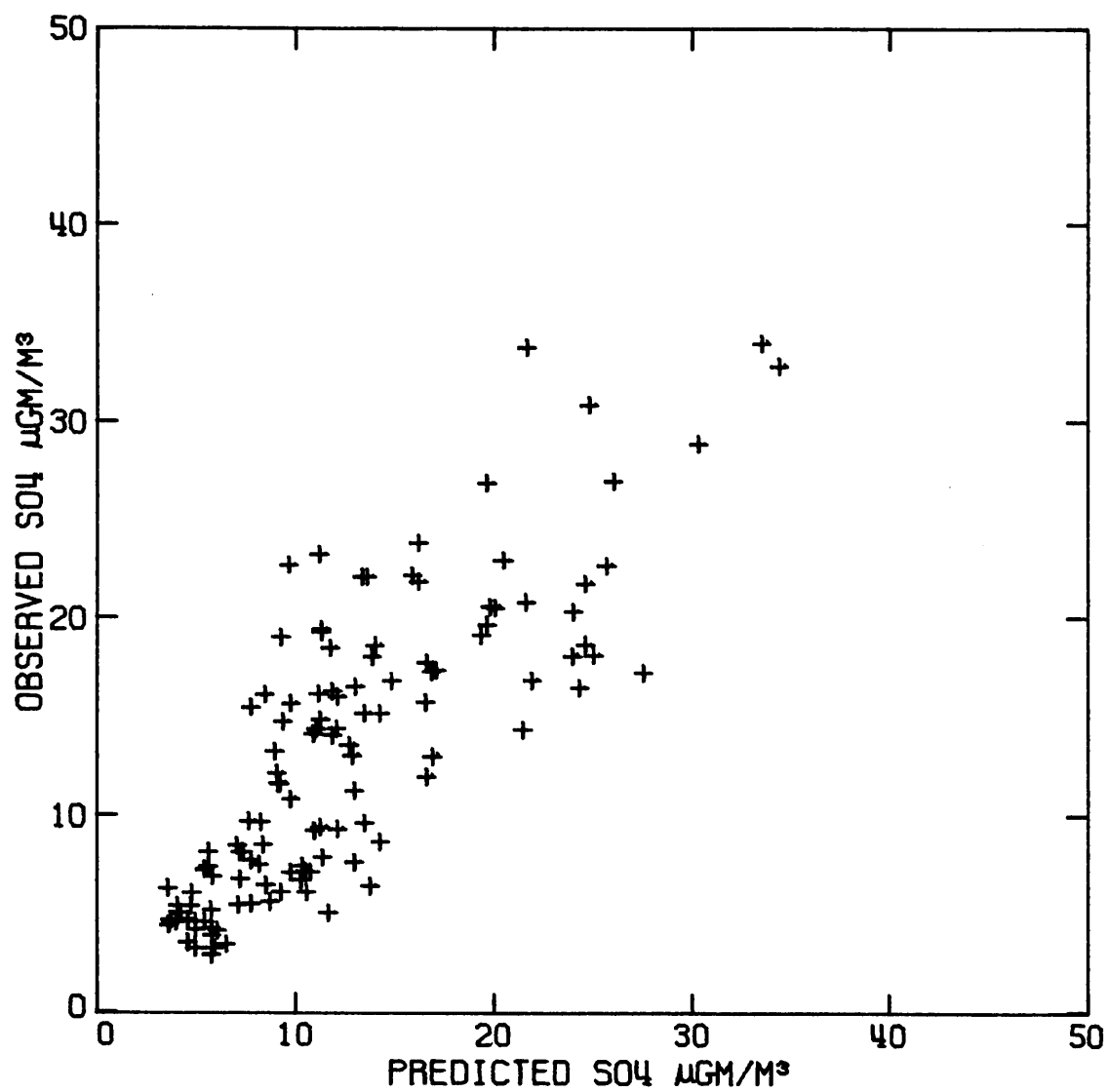
MONTHLY MEANS AT TEN AIR MONITORING STATIONS

FIGURE 5.18

SULFATE AIR QUALITY MODEL RESULTS – 1974
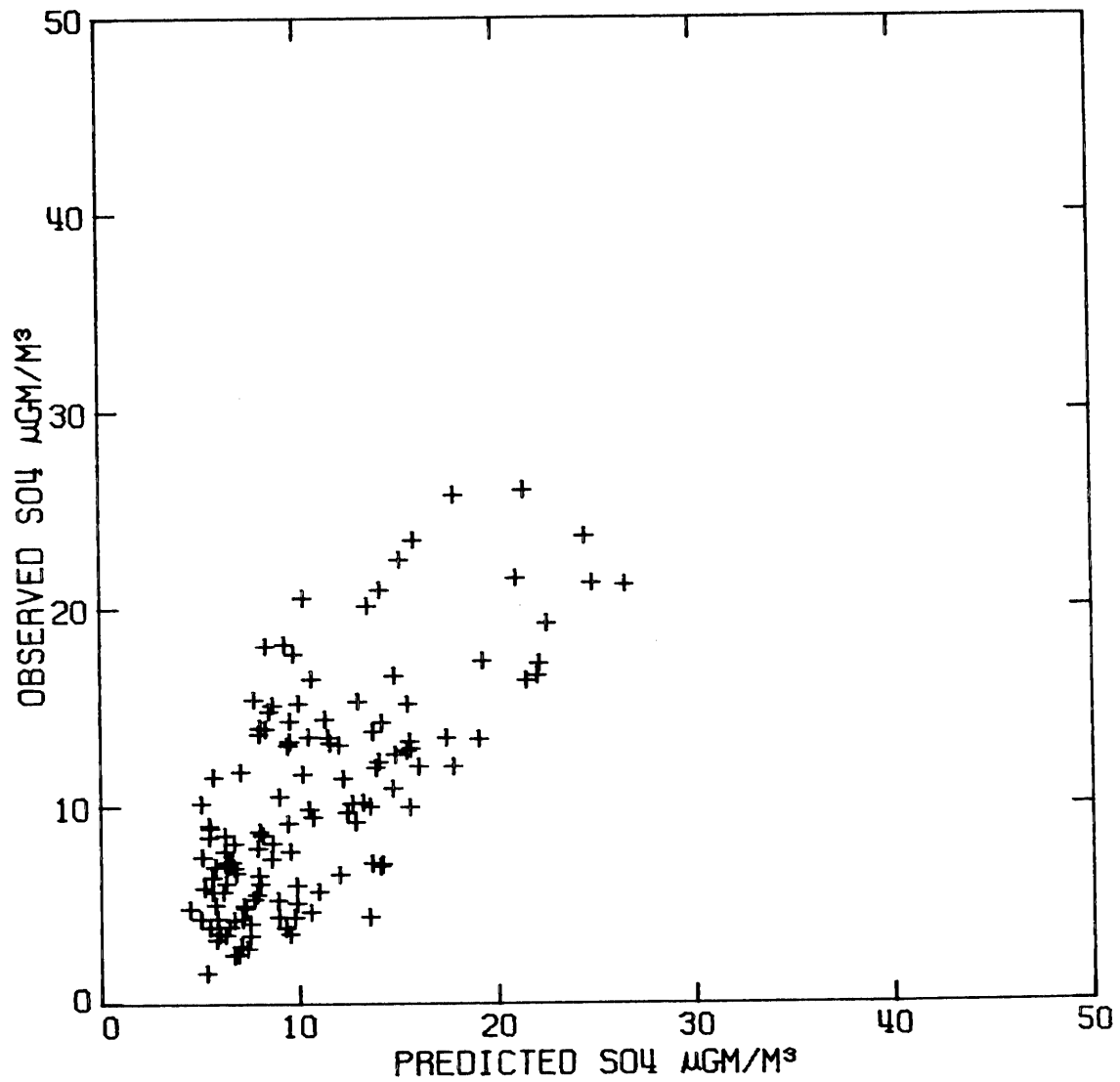
MONTHLY MEANS AT ELEVEN MONITORING STATIONS

FIGURE 5.19

TABLE 5.11

Statistical Comparison of Monthly Average Sulfate Concentrations:
Observations vs. Air Quality Model Results
At Eleven Air Monitoring Sites.

Year	Number of Pairs of Monthly Average Observations and Predictions	Observations		Predictions		Correlation: Observed vs. Predicted
		Mean(b) µgm/m³	Standard Deviation µgm/m³	Mean(b) µgm/m³	Standard Deviation µgm/m³	
1972	108	12.18	5.87	12.51	5.92	0.82
1972(a)	106	12.31	5.84	12.32	5.81	0.89
1973	120	13.12	7.38	12.52	6.80	0.82
1974	128	10.45	5.65	10.80	4.86	0.70

Notes: (a) Biased observations at two CHESS stations discarded for January 1972. These stations did not begin operation until the last four days of that month and thus missed the early January 1972 sulfate episodes. Days sampled were thus not representative of that month.

(b) Unweighted average of available data pairs; because of changing number of days per month and absence of observations at some locations in some months this does not represent an annual mean value.

Correlation analysis alone is a poor measure of model performance. Many air quality models which track temporal trends well fail to accurately reproduce the absolute value of the pollutant concentrations. However, in our case, not only are the observations and predictions highly correlated, but the average values of the predictions and observations are quite close. In addition, the distribution of high and low values throughout the year is closely matched, as shown by the comparison of the standard deviations of the observed and predicted sulfate concentrations given in Table 5.11.

5.4.3 The Seasonal Variation in the Rate of Oxidation of SO_2 to Form Sulfates

Table 5.12 shows the values of the rate of SO_2 oxidation, k, which result from the air quality model application. Each of the entries in that table represents an overall average conversion rate for a particular month. The conversion rates estimated range from a high of 8% per hour to a low of 0.5% per hour.

When SO_2 oxidation rates are averaged horizontally across the columns of Table 5.12, a rather consistent seasonal pattern emerges. Three year average SO_2 oxidation rates are almost exactly 6% per hour from May through September of the year, with no single month in that group more than ±2% per hour above or below the seasonal trend. SO_2 oxidation rates drop sharply in the wintertime. Estimated conversion rates of between 0.5% per hour to 3.0% per hour prevail from October through February.

TABLE 5.12

Calculated Rate of SO_2 Oxidation to Form Sulfates
in the Los Angeles Atmosphere, in Percent per Hour
(Overall Average Values of k for the Month Shown)

Month	1972	1973	1974	Three year mean
January	3%	1%	0.5%	1.5%
February	1%	1.5%	1%	1.2%
March	8%	1%	1%	3.3%
April	3%	5%	1%	3.0%
May	6%	8%	5%	6.3%
June	6%	7%	6%	6.3%
July	4%	8%[a]	5%	5.7%
August	5%	5%	8%	6.0%
September	4%	5%	8%	5.7%
October	2%	1%	3%	2.0%
November	1%	0.75%	1%	0.9%
December	1%	1%	0.5%	0.8%

Notes: (a) Average value from field measurement program in that month.
(Roberts, 1975)

The 8% per hour conversion rate estimated for March 1972 is more

than double the seasonally adjusted average for the month of March.

At k equals 3% per hour, January 1972 also shows a conversion rate

which is double the seasonally adjusted trend for a January month.

Very high sulfate values were observed in early 1972 throughout the

air basin. Weather records at Los Angeles International Airport

(U.S. Department of Commerce, 1972b) indicate that half of

the days of each of those two months were foggy or showed just

enough condensation to yield trace precipitation without a general

washout of the atmosphere. In January 1972, extreme resultant wind

stagnation occurred during a period of high SO_x emissions. That

accounts for the very high sulfate concentrations observed during

January 1972 in spite of the modest (by comparison to summertime) SO_2

oxidation rate.

The 8% per hour SO_2 oxidation rate estimated from Roberts' (1975)

experiments in July 1973 was treated as a predetermined value for that

month. Figure 5.7a shows that a very close fit to observed sulfate

concentrations was obtained at the site of Roberts' experiments in

Pasadena for that month. Such close agreement is probably fortuitous.

But the fact remains that model results are clearly within the range

of observed sulfate concentrations for the only occasion in which

estimates for all parameters in the model are supported by experimental

data.

319

5.4.4 Spatial Variations in Sulfate Air Quality

Figures 5.20 through 5.22 show contour plots of the annual mean
sulfate air quality predictions throughout our study area for each of
the years 1972, 1973 and 1974. A large zone of sulfate-enriched air
is seen to influence most of Los Angeles and northern Orange Counties,
extending from the coastline inland to the San Gabriel Mountains.
Long-term average sulfate concentrations are lower over the ocean and
over the southern portion of Orange County.

In Chapter 2, long-term average sulfate concentrations observed
at local air monitoring stations were found to be rather uniform.
From Figures 5.20 through 5.22 we see that concentration estimates at
most air monitoring stations fall within or near the same contour
interval. However, the simulation model suggests that additional
structure to the sulfate concentration patterns in 1972 and 1973
would have been revealed if a closely spaced network of monitoring sites
had been located downwind of the harbor industrial complex. In 1972,
the highest mean sulfate levels are predicted over South Central Los
Angeles. That pattern was influenced by unusually high sulfate concen-
trations in the winter and early spring of 1972 when inland transport
of pollutants was relatively weak. In contrast, peak sulfate concen-
trations in 1973 are predicted downwind of the harbor industrial complex
in a long corridor which stretches from Carson on the southwest to
beyond the boundaries of our grid system at a point near Pomona on the
northeast. That pattern is due to summertime peak sulfate values in
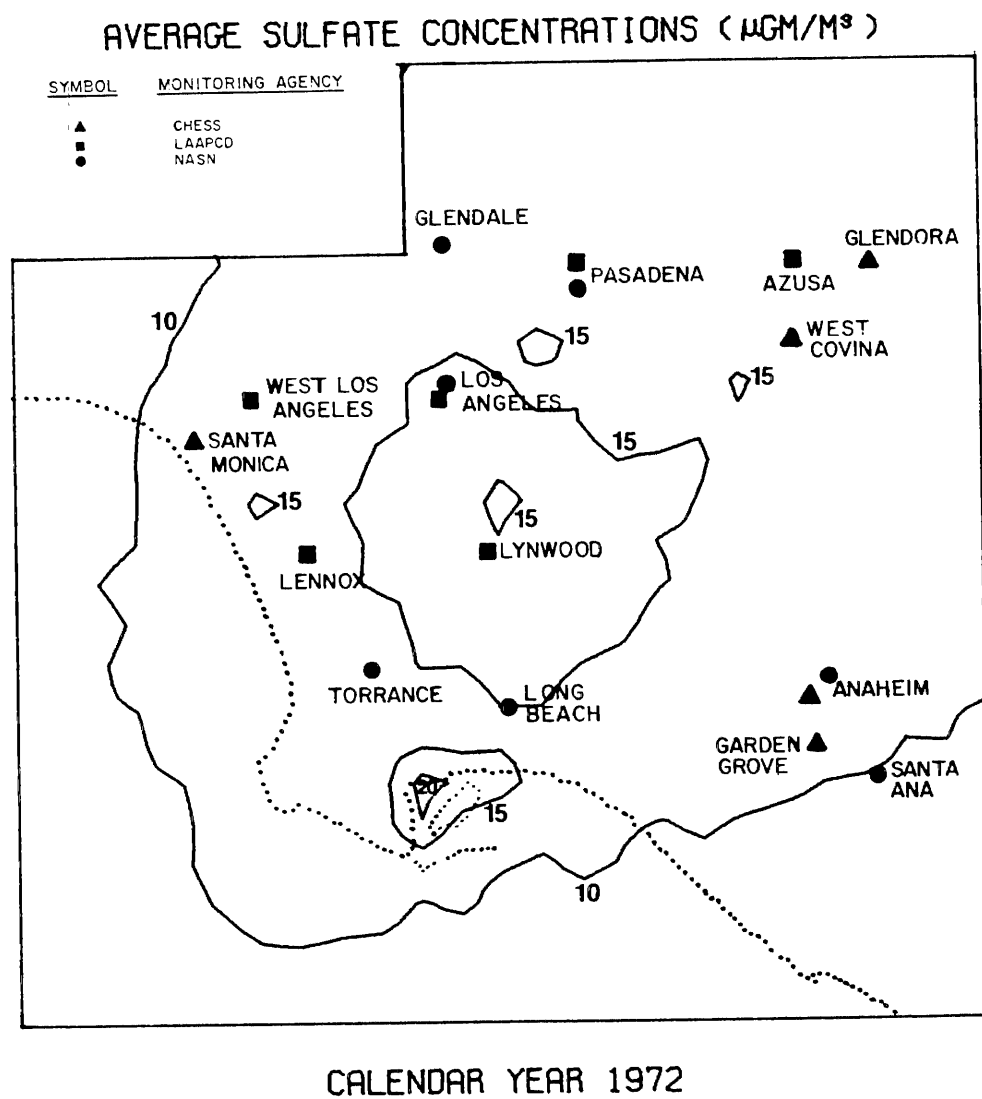1973 which were accompanied by high speed inland transport during the

320

CALENDAR YEAR 1972
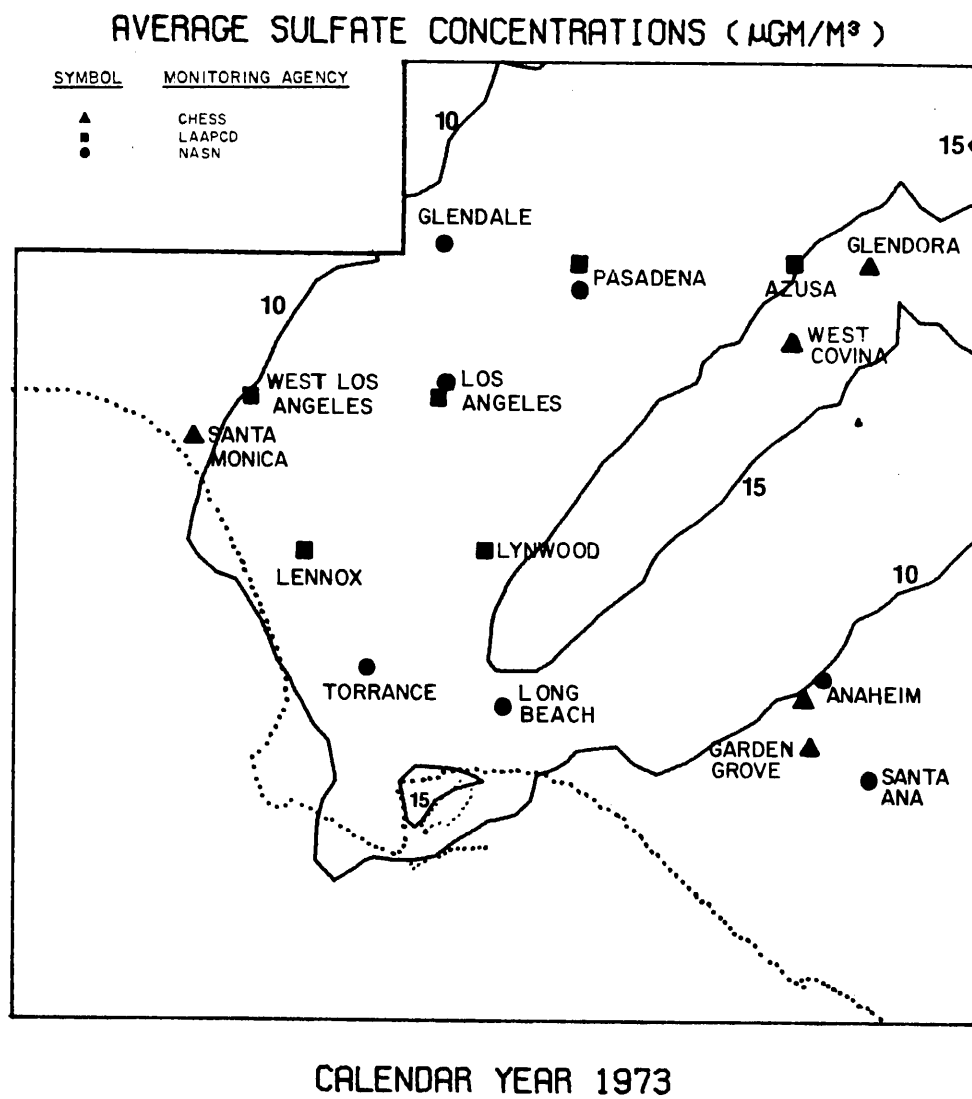
FIGURE 5.20

Annual Mean Sulfate Concentration Isopleths Calculated by the
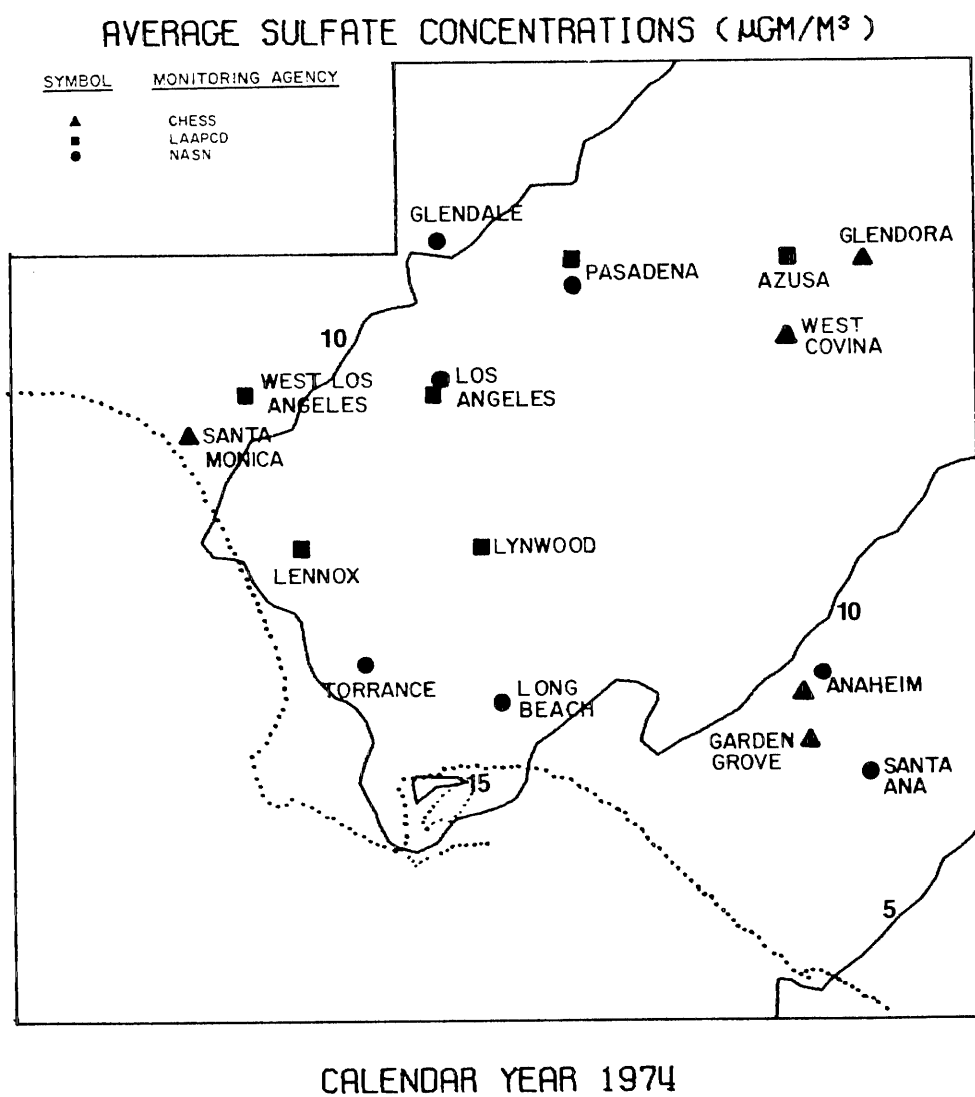Air Quality Simulation Model - 1972

AVERAGE SULFATE CONCENTRATIONS ($\mu GM/M^3$)

SYMBOL   MONITORING AGENCY

▲   CHESS
▪   LAAPCD
●   NASN

GLENDALE

GLENDORA

PASADENA

AZUSA

10

WEST
COVINA

WEST LOS
ANGELES

LOS
ANGELES

SANTA
MONICA

15

LENNOX

LYNWOOD

10

TORRANCE

LONG
BEACH

ANAHEIM

GARDEN
GROVE

SANTA
ANA

15

CALENDAR YEAR 1973

FIGURE 5.21

Annual Mean Sulfate Concentration Isopleths Calculated by the
Air Quality Sumulation Model – 1973

AVERAGE SULFATE CONCENTRATIONS (μGM/M³)

SYMBOL   MONITORING AGENCY

▲   CHESS
■   LAAPCD
●   NASN

GLENDALE

PASADENA

GLENDORA

AZUSA

WEST COVINA

WEST LOS ANGELES

LOS ANGELES

SANTA MONICA

LYNWOOD

LENNOX

10

TORRANCE

LONG BEACH

ANAHEIM

GARDEN GROVE

SANTA ANA

15

5

CALENDAR YEAR 1974

FIGURE 5.22

Annual Mean Sulfate Concentration Isopleths Calculated by the
Air Quality Simulation Model – 1974

afternoon sea breeze regime. This central corridor of highest sulfate

values is absent in 1974, largely because of the control of sulfur

dioxide emissions from some very large chemical plants located just to

the southwest of the start of the 15 $\mu gm/m^3$ sulfate isopleth calculated

in 1973 (see Figure 5.23 and Figure 1.6 in Chapter 1, Section 1.6.1).

In addition, each of our three years of interest shows a small

peak in sulfate concentrations located within the Los Angeles-Long Beach

harbor at Terminal Island. That peak is influenced by fuel burning by

ships in the harbor, as well as by local industries in the harbor area.

To the extent that ships are involved, that peak may be an artifact

of our source class aggregation scheme. All mobile sources were

assigned low effective stack heights when source classes were recombined

for modeling purposes. A ship underway at sea would have a bent-over

plume influenced by the relative velocity between the atmosphere and

the moving ship, while a ship sitting motionless at the dock would have

stack characteristics more closely resembling a small industrial boiler.

Both of these conditions cannot be simulated simultaneously unless our

source classes are subdivided further. An overprediction of the

impact of dockside emissions from ships may have resulted from an

underestimation of their effective stack height. Sulfate air quality

data within the harbor are unavailable, so the presence or absence of

that local enrichment in sulfate levels cannot be confirmed or denied.

Contour plots showing sulfate concentration predictions for each

month of our three year test period are given in Appendix C1. At the

outset, in January and March of 1972, a large sulfate concentration

324

AVERAGE SULFATE CONCENTRATIONS (μGM/M³)

MAJOR SO₂ SOURCES
EMISSIONS OVER 25 TONS/YEAR
▲ STEAM POWER PLANTS
■ OIL REFINERIES
● CHEMICAL PLANTS/
   SULFUR SCAVENGER PLANTS
✗ OTHER SOURCES

CALENDAR YEAR 1973
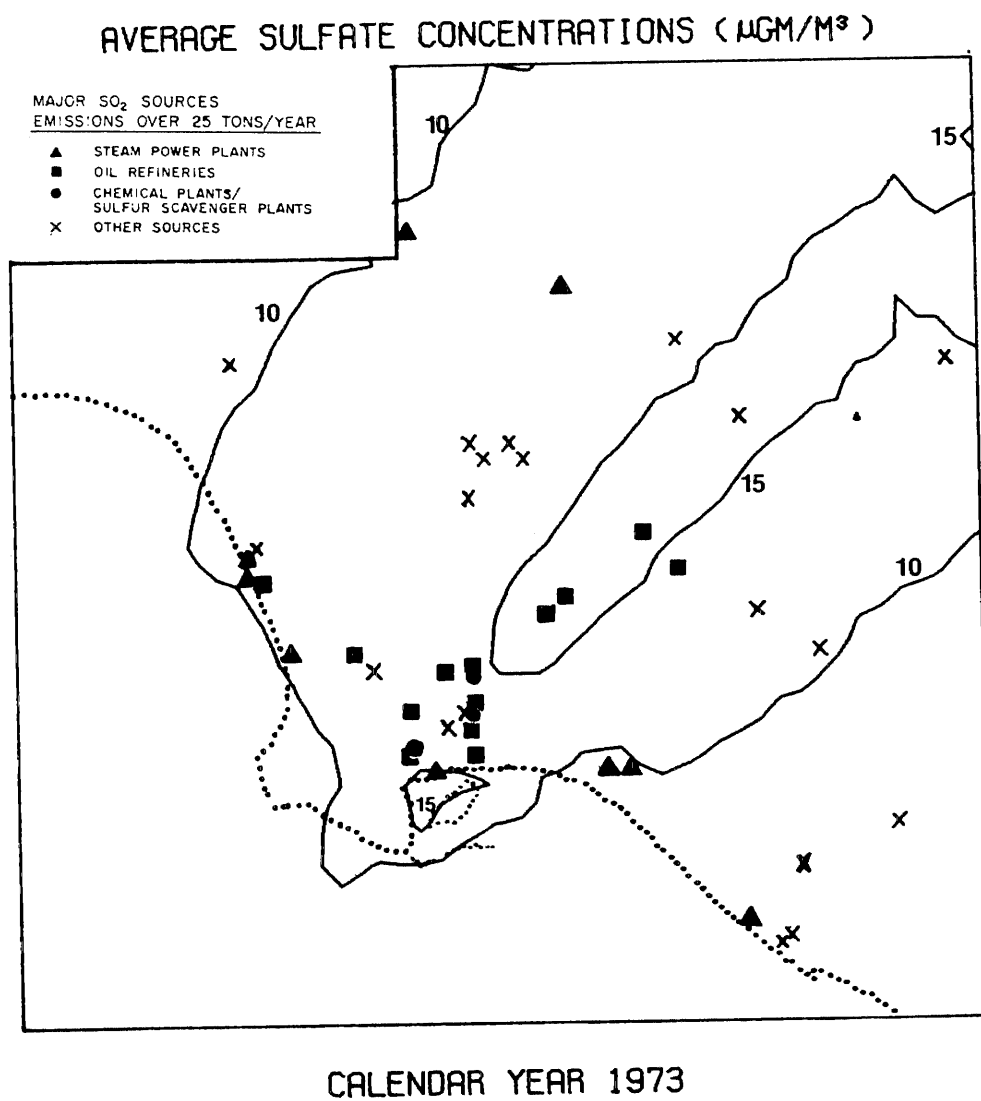
FIGURE 5.23

Annual Mean Sulfate Concentrations in Relation to
Major Point Source Locations - 1973

buildup is noted in the southwest and central portions of Los Angeles County. Our highest sulfate concentration predictions for any month of the three year study period occur during January 1972, with values in several locations in excess of 40 $\mu gm/m^3$ average for the month. That situation occurred because of extended air stagnation in the presence of high SO_2 emissions and a moderate SO_2 oxidation rate estimated at about 3% per hour or less.[5] *While such extended stagnation is unusual, the fact that it can occur means that sulfate air quality control strategy design must consider avoidance of wintertime as well as summertime pollution episodes in Los Angeles.*

The late spring and summer of 1972 are seen to be uneventful. Sulfate concentrations are spread in large dilute air masses, and inland transport causes contours to extend off-grid to the northeast of the major sources in the harbor area. By October 1972, inland transport is stagnating and the SO_2 to sulfate conversion rate is slower. The area affected by sulfate concentrations greater than 10 $\mu gm/m^3$ declines in size and begins to move southwest back toward the harbor area. By December 1972 and January 1973, effective transport is to the seaward side of the air basin, and the inland valleys are nearly drained of their usual pollutant burden.

By April 1973, the cycle has reversed and transport is occurring inland toward Pomona and the Eastern San Gabriel Valley from the coastal

---

[5]Under extended stagnation conditions, τ_c = 48 hours may not be long enough to capture all of the particles contributing to observed air quality. In that case our estimate of k equals 3% per hour would be raised artificially in order to capture the difference.

326

industrial complex. This year, the SO_2 to sulfate conversion rate is a few percent per hour faster than in the summer of 1972, and noticeable areas of elevated sulfate concentrations extend downwind from major source locations at the coast. Monthly mean sulfate concentrations in excess of 30 $\mu gm/m^3$ appear in the Eastern San Gabriel and Pomona-Walnut Valleys in mid-summer. In October 1973, the SO_2 oxidation rate drops and sulfate concentrations decline. By December 1973, the Eastern San Gabriel Valley is largely free of sulfates, and transport appears to have shifted pollutants to the south and west. During 1974, the seasonal cycle observed in 1973 largely repeats itself.

The relatively uniform upwind/downwind annual mean sulfate concentration patterns observed over our three years of interest result in part from a seasonal cycle in which peak sulfate concentrations appeared far inland during the summer and near the coast during the winter.

5.4.5 The Relationship Between Sulfate Air Quality and Total Sulfur Oxides Concentrations

In Chapter 2 it was shown that measured values of the ratio of particulate sulfur oxides to total sulfur oxides, f_s, varied widely from one monitoring network to another. Systematic errors were found to arise from difficulties in measurement of very low sulfur dioxide levels. From a discussion of the nature of those sampling problems, it was suggested that SO_2 data sets at CHESS and LAAPCD stations are likely to be biased *in opposite directions*. Thus all that could be said is that model results for the ratio of sulfates to total sulfur

oxides should fall below the average f_s values from the CHESS and NASN networks, but at or above the typical f_s values calculated from LAAPCD data.

Simulation model results for the ratio of average sulfate to average total sulfur are analyzed in Appendix C2. The air quality simulation tracks the observed seasonal trends in $f_{\overline{s}}$. Model results fall between the bounds established by the CHESS and LAAPCD monitoring data, as expected.

A search was conducted for monitoring sites in the vicinity of major SO_2 sources. The intent was to find locations impacted by high enough SO_2 levels that SO_2 instrument detection limit problems would be minimized. The only such site with both SO_2 and sulfate data is the LAAPCD station at Lennox. Agreement between model results for $f_{\overline{s}}$ and observations at Lennox are excellent. On a few occasions during 1973, sulfur ratio predictions can be compared to high quality field data from the ACHEX study (Hidy, et al., 1975). Again, reasonable agreement is obtained.

Total SO_x concentrations at downtown Los Angeles appear to be overestimated by the model. That problem is thought to arise from mobile source emissions from within the grid cell containing the monitoring site, particularly from an imprecisely inventoried railroad switching yard. With that exception, predicted values of the ratio of particulate sulfur oxides to total sulfur oxides are found to closely reproduce those monitoring results which are free of minimum detection

limit problems, and to fall to the expected side of measurements at stations with significant monitoring biases.

5.4.6   Atmospheric Sulfur Balance Calculations

One advantage of our simulation model is that it maintains a mass balance on the fate of pollutant emissions from each source class. Sulfur oxides are present as SO_2 or as sulfates either within the mixed layer next to the ground or within the elevated inversion, until they have deposited at the ground. By averaging over the pollutant mass balances on emissions from various source types, we may study the long-range effect of source characteristics such as an elevated stack height or a high fraction sulfates in a source's exhaust.

Tables 5.13 through 5.15 show mass balance calculations on SO_x emissions from each source class during one month drawn from each of our three years of interest. A variety of SO_2 oxidation rates and meteorological conditions are represented. The mass balance results summarize a moving average over the outstanding status of all SO_x containing air parcels released from each source during the past 48 hours. The result is similar to examining a flow reactor with a retention time of 48 hours and then averaging over its contents. These calculations differ from those of Roberts (1975, see Figure 2.17) because he established fluxes entering and leaving the boundaries of the airshed over a shorter period of time.

One of the most interesting features revealed by Tables 5.13 through 5.15 is that source effective stack height makes little

TABLE 5.13

Sulfur Balance on Emissions from Each Major Source Class for January 1972

Source Class	Stack Parameters at Reference Conditions		Fraction SO_3 in Exhaust f_{SO_3} (Percent)	Fate of SO_x Emissions Averaged over All On-Grid and Off-Grid Air Parcels Aged Two Days or Less (Percent in Category Shown)					
	Stack Height H (m)	Plume Rise ΔH (m)		SO_2 within mixed layer	SO_4 within mixed layer	SO_2 above mixed layer	SO_4 above mixed layer	SO_2 deposited at ground level	SO_4 deposited at ground level
Electric Utilities	68.6	250.6	3%	18.5	19.1	22.7	21.2	17.7	0.6
Other Fuel Burning Sources	30.5	54.9	3%	20.9	19.5	16.2	17.5	24.9	0.7
Chemical Plants	41.2	36.6	0.6%	21.4	18.5	16.4	16.8	26.0	0.6
Refinery Processes	37.2	164.6	2.8%	20.4	19.9	18.4	18.4	22.0	0.7
Petroleum Coke Kilns	45.7	384.4	8.4%	14.0	17.1	28.1	28.7	11.5	0.5
Glass Furnaces	22.9	44.8	18%	17.7	25.1	13.5	21.0	21.4	1.0
Metals Furnaces	16.8	33.5	1%	21.3	18.5	16.0	16.7	26.6	0.6
Off-Grid Steel Mill	72.5	129.8	2.5%	20.7	19.8	17.9	18.0	22.6	0.7
Misc. Stationary Sources	10.7	21.3	2.8%	20.8	19.0	15.3	16.9	27.2	0.7
Autos and Light Trucks	Surface mixed layer		0.3%	19.9	15.9	13.6	14.9	34.8	0.6
Other Mobile Sources	Surface mixed layer		2.5%	18.3	15.4	10.0	12.8	42.4	0.8

Important Characteristics of that Month:

(a) Average SO_2 Oxidation Rate = 3% per hour

(b) Average $SO_4^=$ Concentration = 25 µgm/m^3

TABLE 5.14

Sulfur Balance on Emissions from Each Major Source Class
for July 1973

Source Class	Stack Parameters at Reference Conditions		Fraction SO_2 in Exhaust f_{so} (Percent)	Fate of SO_x Emissions Averaged over All On-Grid and Off-Grid Air Parcels Aged Two Days or Less (Percent in Category Shown)					
	Stack Height H m	Plume Rise ΔH m		SO_2 within mixed layer	SO_4 within mixed layer	SO_2 above mixed layer	SO_4 above mixed layer	SO_2 deposited at ground level	SO_4 deposited at ground level
Electric Utilities	68.6	250.6	3%	14.5	42.1	5.2	16.6	19.9	1.5
Other Fuel Burning Sources	30.5	54.9	3%	15.7	41.3	2.9	14.4	23.9	1.5
Chemical Plants	41.2	36.6	0.6%	16.1	40.4	2.9	14.1	24.8	1.5
Refinery Processes	37.2	164.6	2.8%	15.4	41.8	3.8	15.3	22.0	1.5
Petroleum Coke Kilns	45.7	384.4	8.4%	11.6	40.4	8.1	23.3	15.1	1.4
Glass Furnaces	22.9	44.8	18%	13.3	46.4	2.4	15.4	20.5	1.8
Metals Furnaces	16.8	33.5	1%	16.1	40.3	2.7	13.9	25.1	1.5
Off-Grid Steel Mill	72.5	129.8	2.5%	15.5	41.6	3.6	15.0	22.5	1.5
Misc. Stationary Sources	10.7	21.3	2.8%	15.8	40.9	2.6	14.0	24.9	1.5
Autos and Light Trucks	Surface mixed layer		0.3%	15.8	40.3	3.5	14.9	23.7	1.5
Other Mobile Sources	Surface mixed layer		2.5%	15.8	40.7	2.6	13.9	25.1	1.5

Important Characteristics of that Month:

(a) Average SO_2 Oxidation Rate = 8% per hour

(b) Average $SO_4^=$ Concentration = 29 μgm/m³

TABLE 5.15

Sulfur Balance on Emissions from Each Major Source Class
for July 1974

Source Class	Stack Parameters at Reference Conditions		Fraction SO_3 in Exhaust f_{SO} (Percent)	Fate of SO_x Emissions Averaged over All On-Grid and Off-Grid Air Parcels Aged Two Days or Less (Percent in Category Shown)					
	Stack Height H m	Plume Rise ΔH m		SO_2 within mixed layer	SO_4 within mixed layer	SO_2 above mixed layer	SO_4 above mixed layer	SO_2 deposited at ground level	SO_4 deposited at ground level
Electric Utilities	68.6	250.6	3%	15.8	28.4	12.2	21.0	21.3	1.1
Other Fuel Burning Sources	30.5	54.9	3%	17.5	27.1	7.4	17.3	29.3	1.1
Chemical Plants	41.2	36.6	0.6%	18.0	25.8	7.1	16.5	31.2	1.1
Refinery Processes	37.2	164.6	2.8%	16.8	28.0	10.2	19.5	24.1	1.1
Petroleum Coke Kilns	45.7	384.4	8.4%	12.4	26.4	16.3	28.6	15.2	0.9
Glass Furnaces	22.9	44.8	18%	14.8	32.5	5.9	19.2	25.7	1.5
Metals Furnaces	16.8	33.5	1%	17.9	25.6	6.7	16.2	32.3	1.1
Off-Grid Steel Mill	72.5	129.8	2.5%	17.0	28.1	9.9	19.1	24.5	1.1
Misc. Stationary Sources	10.7	21.3	2.8%	17.6	26.2	6.5	16.4	31.9	1.1
Autos and Light Trucks	Surface mixed layer		0.3%	17.6	25.5	8.1	17.5	29.9	1.1
Other Mobile Sources	Surface mixed layer		2.5%	17.5	25.7	6.1	15.9	33.4	1.1

Important Characteristics of that Month:

(a) Average SO_2 Oxidation Rate = 5% per hour

(b) Average $SO_4^=$ Concentration = 12 $\mu gm/m^3$

difference to the amount of sulfate appearing in the ground level mixed layer during a two day period. Petroleum coke kilns with their very high effective stack heights succeed in forcing an unusually large amount of their emissions above the mixed layer into the elevated inversion. While this shields emissions from ground level temporarily, it also suppresses SO_2 deposition at the ground by a compensating amount. Receptor points close to the source will benefit from this treatment while those farther downwind will not.

Ground level mobile SO_2 sources ultimately achieve slightly lower sulfates mass loadings during the winter through enhanced SO_2 deposition under conditions of surface-based inversion. Since SO_2 concentration is the driving force for SO_2 dry deposition, this slight reduction in airborne sulfate mass over the long-term is being achieved at the expense of creating higher than usual SO_2 concentrations per ton of emissions. Ground level release of pollutants is not an acceptable route to sulfate air quality control. It does not result in much of a sulfate mass reduction and is likely to create an SO_2 or primary SO_3 concentration problem close to the source.

The effect of a high fraction sulfates in an elevated source's exhaust can be examined by comparing glass furnaces to metals furnaces. The plume rise characteristics of these source classes are similar, but the glass furnaces release about 18% of their SO_x emissions as SO_3 or sulfates. The result is a definite enrichment in sulfates within the mixed layer as compared with a source with lower primary sulfates emissions. This discussion is not intended to single out glass furnaces

as being particularly offensive, since glass furnaces represent a very small fraction of the basin's SO_x emission inventory. The objective is to show that primary SO_3 or sulfates emissions from any source should be avoided if possible.

It is concluded that for the historic cases examined here, source specific characteristics such as plume rise or fraction SO_3 in a source's exhaust have played a relatively minor role in determining differences between the _mass_ of sulfate contributed by various source classes. The amount of sulfate residing in the mixed layer is most directly related to SO_x emission strength and SO_2 oxidation rate. In addition, the _concentration_ of sulfate observed in the air basin depends as much on transport patterns and source location as on reaction rate. The total amount of sulfate found during July 1973 at k = 8% per hour within our hypothetical flow reactor is about double the amount formed in January 1972 at k = 3% per hour. The average sulfate concentrations observed in those two months were comparable because a higher fraction of total SO_x emissions stagnated close to their source in January than in July.

5.4.7 Source Class Contributions to Sulfate Air Quality

Contour plots of individual source class contributions to sulfate air quality can help to explain how the air basin becomes so nearly filled by sulfate concentrations of the same general magnitude while emissions remain concentrated in a handful of locations. In many months with a pronounced daily sea breeze/land breeze wind reversal,

air parcel trajectories wander widely over the basin. Sulfur oxides
are dispersed within the airshed by the rotation of the wind vectors
over time, much as a person stands in the center of his garden and
waters the lawn by spraying a hose from side to side. Contours of
average sulfate concentration from even the largest point sources
can become an amorphous blob under such circumstances as shown in
Figures 5.24 through 5.31. It is therefore not surprising that super-
position of many such shapeless air quality impacts centered on
different source locations leads to a nondescript average sulfate
loading of the airshed in such months.

In contrast during the summer, onshore wind flow persists for most
of the day. Similar air parcel trajectories are repeated from day to
day. Distinct zones of major source influence stretch inland from the
coast.

The impact of the power plant complexes at El Segundo and at
Alamitos Bay is clearly evident in Figure 5.32. The El Segundo area
generating stations lie at the head of a sulfate enrichment which
typically passes over downtown Los Angeles and continues inland toward
Pasadena in the summer. Emissions from the Alamitos Bay area are
predicted to typically pass along the Los Angeles County-Orange County
border, through La Mirada, La Habra, and Diamond Bar, and then out the
Pomona-Walnut Valley.

Upwind-downwind sulfate concentration gradients along the transport
paths downwind of these power plants are fairly small. Lateral

335

SULFATE AIR QUAILTY INCREMENT DUE TO

ELECTRIC UTILITY BOILERS (µGM/M³)
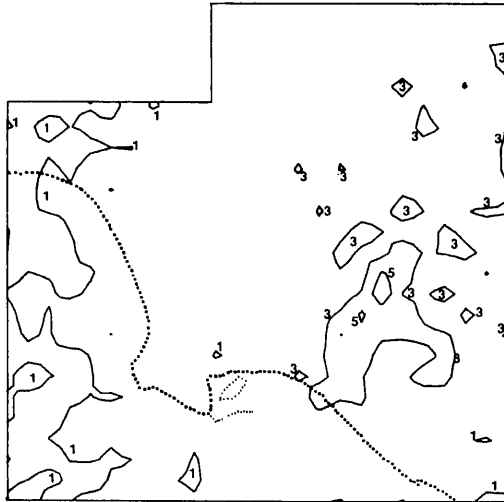
FEBRUARY 1972

FIGURE 5.24

SULFATE AIR QUAILTY INCREMENT DUE TO

OTHER FUEL BURNING SOURCES (µGM/M³)
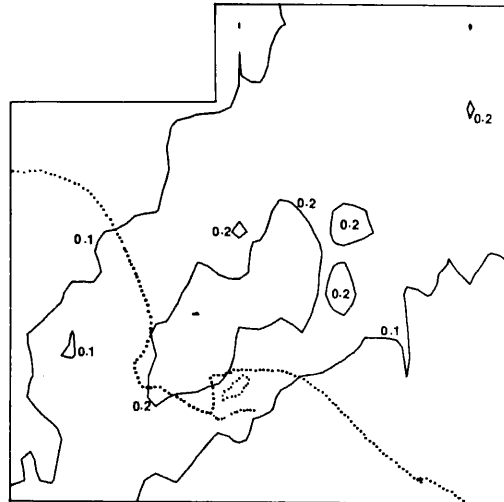
FEBRUARY 1972

FIGURE 5.25

SULFATE AIR QUAILTY INCREMENT DUE TO

CHEMICAL PLANTS (µGM/M³)
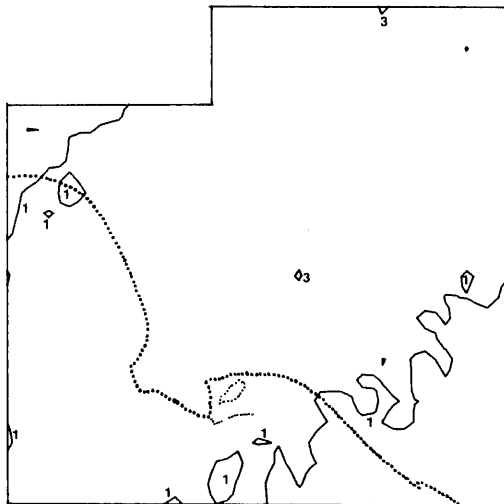
FEBRUARY 1972

FIGURE 5.26

SULFATE AIR QUAILTY INCREMENT DUE TO

PETROLEUM INDUSTRY PROCESSES (µGM/M³)
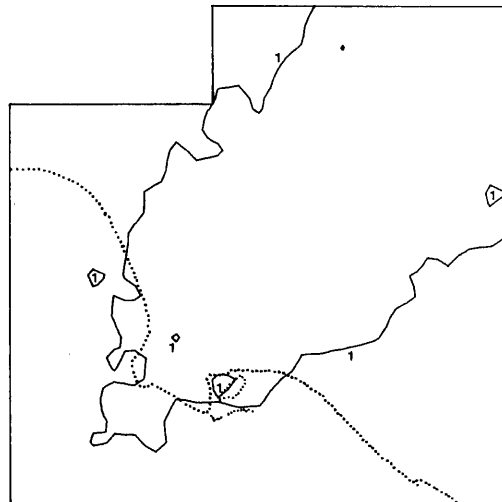
FEBRUARY 1972

FIGURE 5.27

336

SULFATE AIR QUAILTY INCREMENT DUE TO

MISCELLANEOUS STATIONARY SOURCES (µGM/M³)
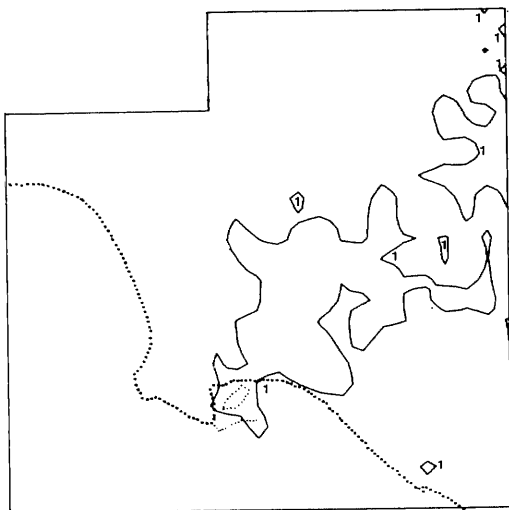
FEBRUARY 1972

FIGURE   5.28

SULFATE AIR QUAILTY INCREMENT DUE TO

AUTOS AND LIGHT TRUCKS (µGM/M³)
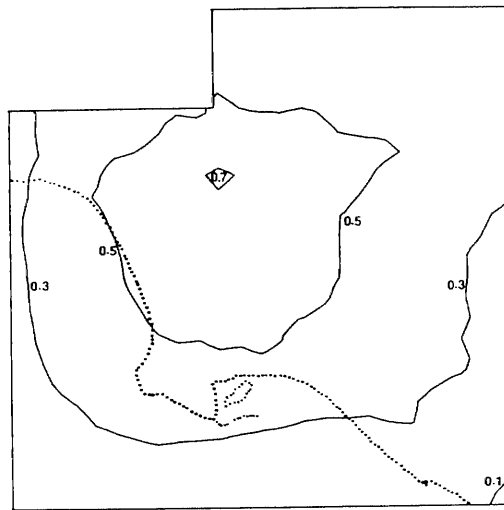
FEBRUARY 1972

FIGURE   5.29

SULFATE AIR QUAILTY INCREMENT DUE TO

OTHER MOBILE SOURCES (µGM/M³)
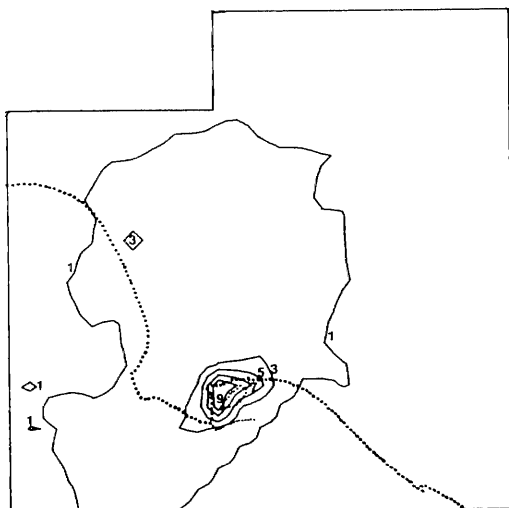
FEBRUARY 1972

FIGURE   5.30

SULFATE AIR QUAILTY INCREMENT DUE TO

ALL SOURCES PLUS BACKGROUND (µGM/M³)
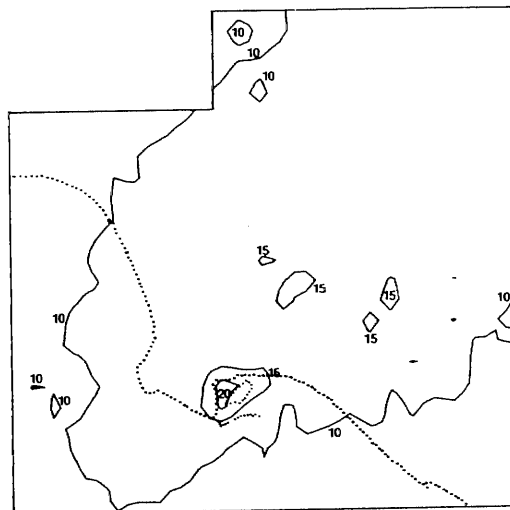
FEBRUARY 1972

FIGURE   5.31

SULFATE AIR QUAILTY INCREMENT DUE TO

ELECTRIC UTILITY BOILERS (μGM/M³)
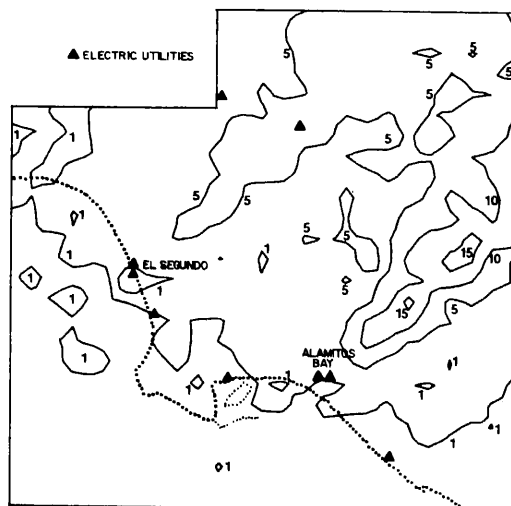
JULY 1973

FIGURE 5.32

SULFATE AIR QUAILTY INCREMENT DUE TO

OTHER FUEL BURNING SOURCES (μGM/M³)
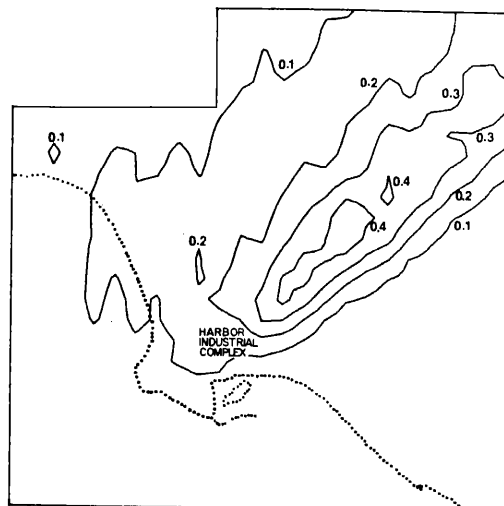
JULY 1973

FIGURE 5.33

SULFATE AIR QUAILTY INCREMENT DUE TO

CHEMICAL PLANTS (μGM/M³)
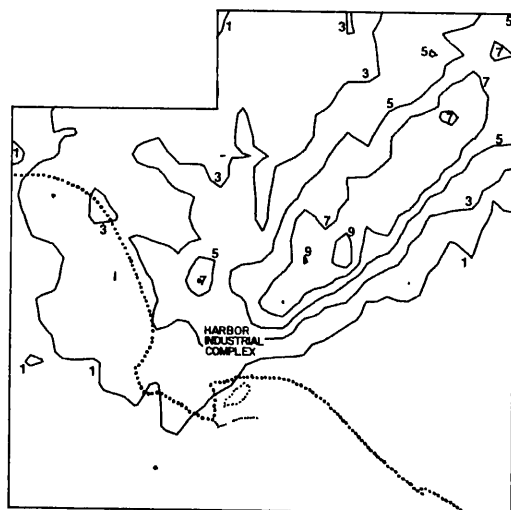
JULY 1973

FIGURE 5.34

SULFATE AIR QUAILTY INCREMENT DUE TO

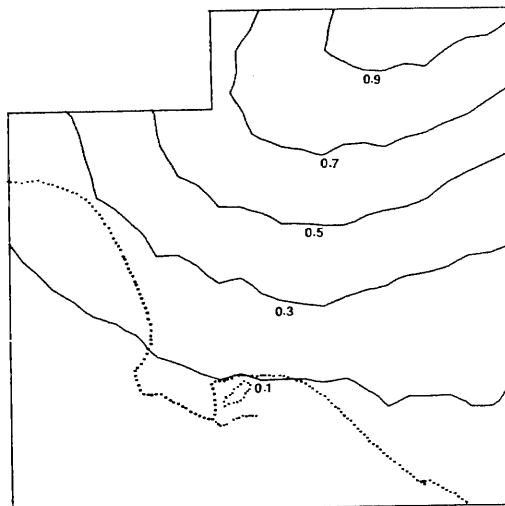PETROLEUM INDUSTRY PROCESSES (μGM/M³)
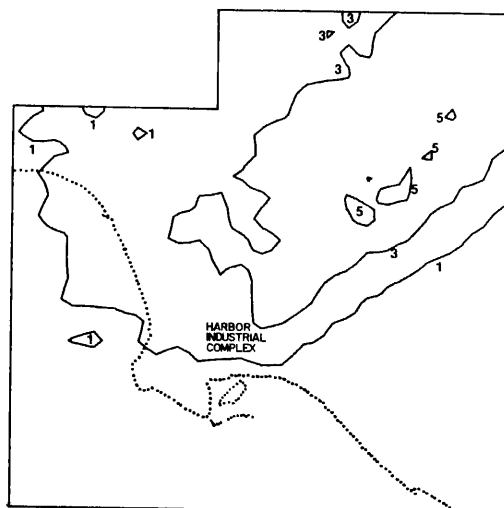
JULY 1973

FIGURE 5.35

338

SULFATE AIR QUAILTY INCREMENT DUE TO

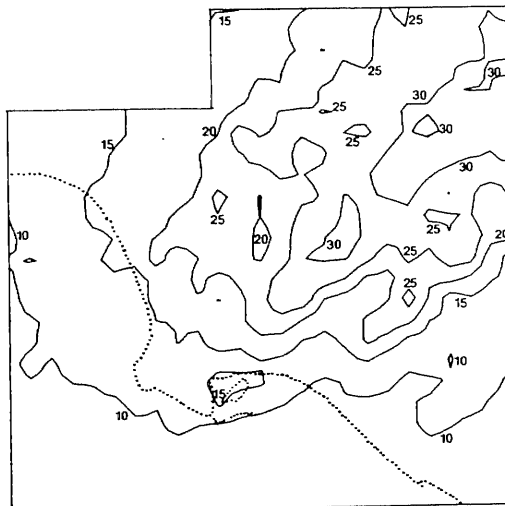MISCELLANEOUS STATIONARY SOURCES (μGM/M³)
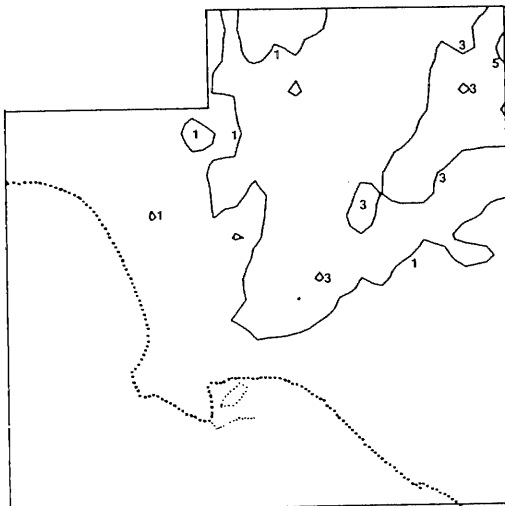
JULY 1973

FIGURE 5.36

SULFATE AIR QUAILTY INCREMENT DUE TO

OTHER MOBILE SOURCES (μGM/M³)

JULY 1973

FIGURE 5.38

SULFATE AIR QUAILTY INCREMENT DUE TO

AUTOS AND LIGHT TRUCKS (μGM/M³)

JULY 1973

FIGURE 5.37

SULFATE AIR QUAILTY INCREMENT DUE TO

ALL SOURCES PLUS BACKGROUND (μGM/M³)

JULY 1973

FIGURE 5.39

spreading acts to reduce sulfate concentrations at a rate nearly sufficient to counteract sulfate formation.

The sulfate enrichment zones downwind of major point sources in July of 1973 are predicted to have a shape which resembles a plume over the long-term average. It should be noted however that the model does not presuppose a plume-like structure, and that in fact the existence of a definite plume from these sources is probably intermittent. Long-term average concentration patterns which resemble a plume trace can be achieved by permitting stagnation of pollutants in the morning, followed by transport of a well-aged air mass across the basin during the day in a way that passes over successive receptor points downwind in a relatively straight line.

The air parcel trajectory calculations within our simulation model were performed by a very approximate method. It is highly possible that source to receptor transport pairs could be misaligned somewhat as a result. However, power plant pollutant transport patterns like those of Figure 5.32 can be checked against the more detailed transport calculations of others with some success. Mid-day and afternoon pollutant transport patterns are heavily weighted when computing the air quality impact of power plant emissions. That is because the diurnal variation of power plant emissions peaks strongly at that time. Drivas and Shair (1975) marked an Alamitos Bay power plant plume with a conserved tracer on numerous mornings and afternoons during October 1973. In nearly every case sampled, Drivas and Shair located that plume within the area indicated by our simulation model.

The gap between the Alamitos Bay and El Segundo area power plant impacts during the summer is filled by the effluent from industries in the harbor area. The major point sources in that area are chemical plants, refinery process operations and petroleum coke calcining kilns.

Automotive emissions are distributed throughout the airshed. As a result, there is little opportunity for effective lateral dispersion of emissions from the source class as a whole. The sulfate air quality impact of automotive emissions becomes more intensive downwind as chemical reactions cause sulfate concentrations to increase within a large dilute air mass. The net transport differences between summer and winter are clearly evident when comparing Figure 5.29 to Figure 5.37. In summer the sulfate peak from downtown traffic is pushed far inland, while in winter, peak concentrations from automobiles occur in west central Los Angeles.

Figures 5.6(b) through 5.16(b) show the source class increments to sulfate air quality calculated at all CHESS and LAAPCD monitoring stations in time series. Those graphs were purposely presented along-side of the comparison of model results to observed sulfate concentra-tions. This was done so that the reader can easily identify situations where model predictions fall short of observations and thus where sulfate contributions from other unspecified sources are indicated. Source class increments to sulfate levels at NASN monitoring sites are shown in Figures 5.40 through 5.43. NASN stations at downtown Los Angeles, Pasadena and Anaheim are not presented since predictions at

SOURCE CLASS CONTRIBUTION TO SULFATE CONCENTRATIONS
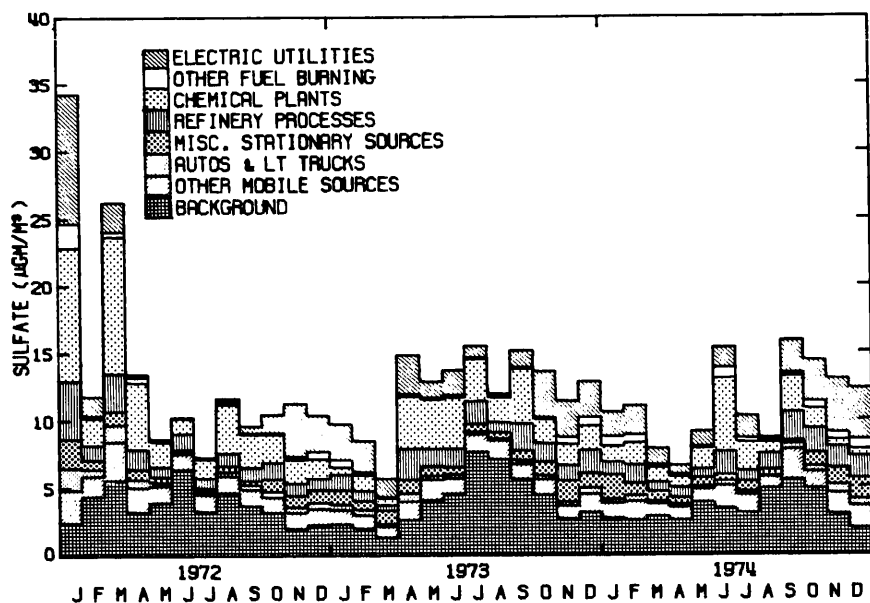
OBSERVED AT TORRANCE (NASN)

FIGURE 5.40

SOURCE CLASS CONTRIBUTION TO SULFATE CONCENTRATIONS
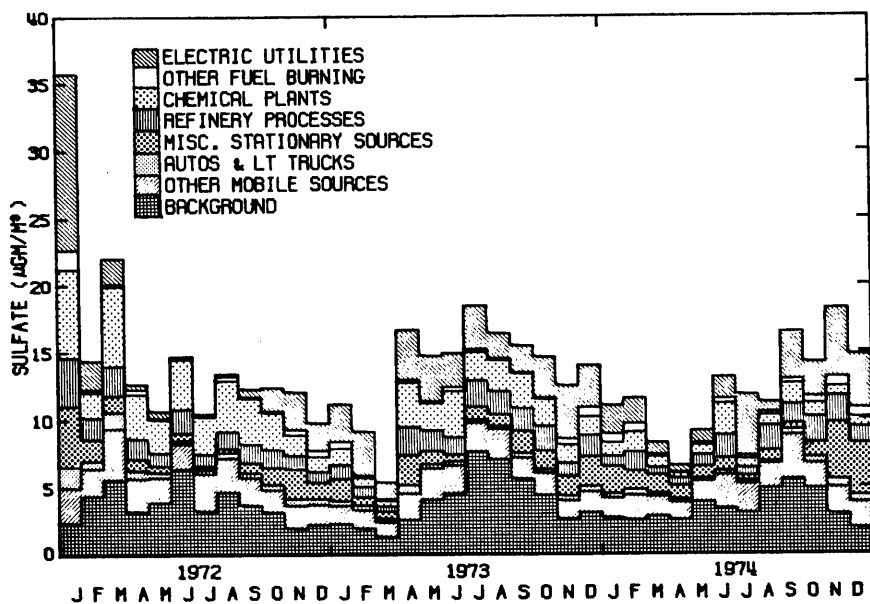
OBSERVED AT LONG BEACH (NASN)

FIGUFE 5.41

SOURCE CLASS CONTRIBUTION TO SULFATE CONCENTRATIONS
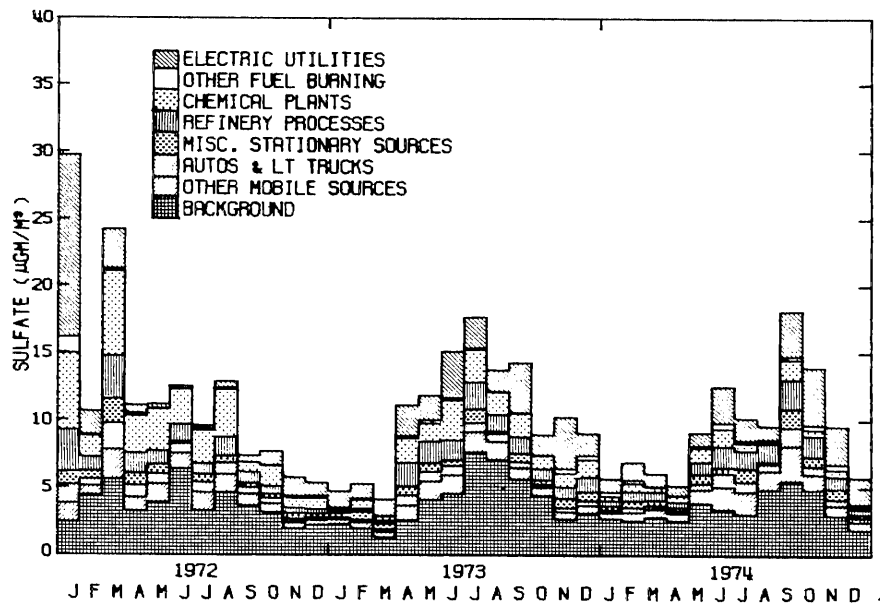
OBSERVED AT GLENDALE (NASN)

FIGURE   5.42

SOURCE CLASS CONTRIBUTION TO SULFATE CONCENTRATIONS
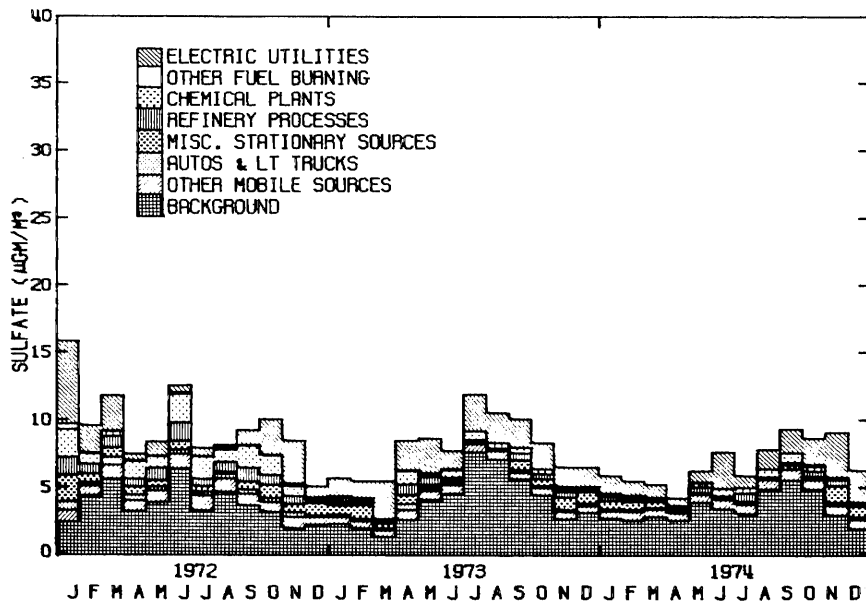
OBSERVED AT SANTA ANA (NASN)

FIGURE   5.43

those locations are substantially the same as at the CHESS or LAAPCD monitoring sites of the same name.

Three to five source classes of about equal impact, plus background sulfates, must be considered simultaneously in order to come close to explaining observed sulfate levels at most locations. The main lesson drawn from these source class contribution estimates is that no single source class dominated sulfate air quality in the Los Angeles Basin during our study period.

Within the last few years, a number of investigators of Los Angeles sulfate air quality have attempted to deduce source to receptor influence relationships for sulfates by regression analysis of emissions and air quality data (Heisler, 1976; Joint Project 1977; White, et al., 1978). Great difficulty was encountered in formulating and validating empirical emissions-air quality relationships that would assist sulfate pollution control strategy analysis. The reason is now fairly clear. Referring to Figure 4.8, we see that most of the source classes responsible for observed sulfate levels have so little variance in their emissions patterns over time that it would be impossible to explain the wide variance in observed air quality on the basis of variance in emissions alone.

The only sources with large well-defined short-term fluctuations in emissions are power plants, and they do not account for enough of the total sulfate burden to dominate the variance in ambient sulfate air quality. However, using statistical techniques plus the lack of a strong correlation between power plant emissions and observed air

quality, White, et al. (1978) derived an upper limit estimate for the contribution of power plant emissions to sulfate air quality at West Covina. They determined that power plant emissions accounted for no more than 17% of the sulfate burden at that location. Our model results at West Covina do not conflict with that estimate. The power plant impact calculated from our simulation model accounts for 17.4% of the total sulfate loading at West Covina, averaged over three years.[6] Power plant impact is proportionately higher elsewhere, however.

It may seem discouraging that no clear cut "cure" for the sulfate problem can be obtained by attacking SO_x emissions from a single source class. However, the situation depicted by the simulation model is not without its positive points. The condition of roughly equal impact from a wide variety of source types leaves the control strategy analyst with the flexibility to generate a wide variety of possibly acceptable emission control strategies. Decision-makers may then choose from among those options on the basis of minimization of emission control costs, flexibility of the control strategy to deal with changing circumstances, or compatibility of the strategy with other simultaneous objectives such as minimization of NO_x emissions or conservation of energy resources.

---

[6]The extremely close agreement of these two estimates is again probably fortuitous. The air quality simulation model is sufficiently complex that we could not have hit a target that closely if we had tried, which we did not.

5.5 Summary

The data requirements of the sulfate air quality simulation model were examined. It was found that the number of virtual emissions sources supplied to the air quality model could be greatly reduced through recombination of sources into eleven broad source classes, and through aggregation of point sources located within a common grid square.

The retention time within the 50 by 50 mile square grid for air parcels released from major point source locations was investigated. It was estimated that 95% of those air parcels would be cleared from the grid system within two days (on an annual average basis). Fluctuations above and below that value will occur from month to month, with generally longer than average retention times in some winter months, and shorter than average retention times in most summer months.

The problem of estimating the rate of horizontal eddy diffusion over urban areas was addressed. Estimates for the standard deviation of horizontal plume spread as a function of travel time downwind, $\sigma_y(t)$, were made based on experimental data taken over the urban areas of St. Louis and Los Angeles.

The seasonal variation of sulfate background air quality in the South Coast Air Basin was examined. It was found that data sufficient to dictate the seasonal pattern in sulfate concentrations in incoming marine air for each month of the period 1972 through 1974 are unavailable. The best estimate that could be made of South Coast Air Basin sulfate background levels was obtained by scaling the seasonal

variation in sulfate air quality observed at the most rural air
quality station influenced by coastal meteorology (at Vista) to the
average magnitude of sulfate concentrations observed at San Nicolas
Island.

The remaining data requirements of the model also were satisfied.
These include selection of deposition velocities for SO_2 and for
sulfates, selection of data on wind speed and direction, and specifi-
cation of inversion base motion over time. It was determined that
the overall rate of SO_2 oxidation to form sulfates would have to be
determined by iteration, and a procedure was outlined for performing
those calculations within a highly over-determined system of equations.
Finally, a time step for trajectory integration and a receptor cell
size were selected.

The air quality dispersion model was applied to Los Angeles
sulfate air quality over each month of the years 1972 through 1974.
It was found that model results closely reproduced observed sulfate
concentration patterns within the central portion of the Los Angeles
Basin, particularly during the years 1972 and 1973. The correlation
between observed and predicted sulfate levels is 0.82 in both 1972
and 1973, and rises to 0.89 in 1972 if two biased observations are
discarded.

A seasonal variation in the overall rate of SO_2 oxidation to form
sulfates in the Los Angeles atmosphere was inferred from the results
of the air quality modeling study. Monthly mean SO_2 oxidation rates

of between 0.5% per hour and 3% per hour prevail from October through

February of our test years. During the late spring, summer and early

fall, SO_2 oxidation rates were estimated to jump to an average of

about 6% per hour, with individual months ranging ± 2% per hour about

that mean value. Those numerical results must be qualified since a

better understanding of seasonal trends in background sulfate concen-

trations or SO_2 deposition velocity might alter the outcome somewhat.[7]

Examination of individual source class contributions to sulfate

air quality can help to explain how the air basin becomes so nearly

filled by sulfate concentrations of the same general magnitude while

emissions sources remain clustered in a handful of locations. In

winter months with a pronounced daily sea breeze/land breeze wind

reversal, sulfur oxides are dispersed within the airshed by the

rotation of the wind vectors. In contrast, during mid-summer, onshore

flow persists for most of the day. Similar air parcel trajectories

are repeated from day to day. However, the sequential siting of

major SO_x sources along the coast means that the central portion of

the air basin is downwind of one major source group or another at most

times. Lateral dispersion of emissions is just about sufficient to bal-

ance sulfate formation, with the result that downwind and crosswind

pollutant gradients are rather small in spite of the direct inland

---

[7]For a sensitivity study of conversion rate calculation dependence on
other airshed parameters, see Roberts (1975).

transport from sources to receptors. Annual mean sulfate concentrations are further smoothed by seasonal transport cycles in which peak sulfate concentrations appeared far inland during the summer and near to the coast during the winter.

In January 1972, extreme resultant wind stagnation occurred during a period of high SO_x emissions. The highest localized sulfate concentration predictions for any month of our three year period occurred at that time. While such extended stagnation is unusual, the fact that it can occur means that sulfate air quality control strategy design must consider avoidance of wintertime as well as summertime pollution episodes in Los Angeles.

Source class increments to predicted sulfate air quality were examined in time series at each air monitoring station. It was found that three to five source classes of roughly equal impact, plus background sulfates, must be considered simultaneously in order to come close to explaining sulfate levels observed at most locations. The implication is that a mixed strategy targeted at a combination of source types will be needed if significant sulfate air quality improvements are to be achieved in this airshed through precursor SO_x control.